Modeling Brk/PTK6 Expression in the Mammary Epithelium

A DISSERTATION
SUBMITTED TO THE FACULTY OF THE GRADUATE SCHOOL
OF THE UNIVERSITY OF MINNESOTA
BY

Kristopher Andrew Lofgren

IN PARTIAL FULFILLMENT OF THE REQUIREMENTS
FOR THE DEGREE OF DOCTOR OF PHILOSOPHY

Adviser: Carol A. Lange

December 2010

ACKNOWLEDGEMENTS

I would like to gratefully acknowledge the following people:

Dr. Carol Lange for her guidance in multiple facets of science and life.

Lange Lab past and present (particularly Grey Hubbard, Dr. Daniel Housa, and Dr. Julie Ostrander, for direct technical contributions).

Dr. Kaylee Schwertfeger for equipment use, temporary lab space, reagents and input.

Funding for this work was provided by NIH/NCI R01 CA107547 to Carol A. Lange and a Department of Defense Breast Cancer Research Pre-doctoral Fellowship W81XWH-06-1-0752 to Kristopher A. Lofgren

DEDICATION

I would like to dedicate my dissertation to my entire family and wife. Thank you for all of your support and inspiration through the years.

ABSTRACT

Protein tyrosine kinases (PTKs) regulate cellular proliferation and differentiation during development and homeostasis of normal tissues. Additionally, PTKs are frequently overexpressed in cancers. As such, they have become promising targets for new therapies. Breast tumor kinase (Brk/PTK6) is a non-receptor tyrosine kinase initially cloned from a metastatic breast tumor, and is overexpressed in ~86% of human breast tumors and several breast cancer cell lines. While expressed in differentiating cells in the skin and intestine, Brk is notably absent from normal mammary tissue and non-transformed mammary epithelial cell lines. The role of Brk/PTK6 in breast pathology is unclear. We hypothesized that Brk expression in non-transformed mammary epithelium would promote tumorigenesis. To determine the effects Brk expression in the normal mammary gland, we sought to create a mouse model for tissue-specific Brk expression. We expressed a WAP-driven Brk/PTK6 transgene in FVB/n mice, and analyzed wild-type and transgenic mammary glands after forced weaning. Brk-transgenic dams exhibited delayed mammary gland involution and infrequent tumors in aged mice. Transgenic mammary glands displayed decreased STAT3 phosphorylation, a marker of early stage involution. Signaling mediators downstream of Brk, including STAT5 and p38 MAPK were activated relative to wild-type mice. Brk-mediated signaling to STAT5 and p38 MAPK was recapitulated with Brk expression in non-transformed HC11 murine mammary epithelial cells. Additionally, non-transformed HMEC and HC11 cells expressing Brk exhibited increased anchorage-independent survival when cultured on PolyHEMA coated dishes. Samples from breast tumor biopsies were subjected to IHC

analysis for co-expression of Brk, phospho-STAT5, and phospho-p38 MAPK. Ductal and lobular carcinomas expressing Brk exhibited elevated phospho-STAT5 and phospho-p38 MAPK, respectively, whereas non-malignant tissues were Brk-null with dramatically less phospho-STAT5 and phospho-p38 expression. HMEC cells expressing Brk underwent luminal hollowing (reliant on cell death) similar to normal mammary alveologenesis when cultured on Matrigel, but are partially resistant to doxorubicin treatment, suggesting a context dependent component to Brk-mediated survival. HGF, EGF, or IGF treatment in cells that endogenously express Brk (non-transformed HaCaT keratinocytes and MDA-MB-231 breast cancer cells), resulted in growth factor specific changes in Brk localization, but only in MDA-MB-231 cells. Brk-knockdown in breast cancer cells (T47D and SKBR3) identified differential phosphorylation of Erk5, and notably, p38 MAPK in response to EGF and heregulin-β1 treatment. These studies illustrate that forced expression of Brk/PTK6 in non-transformed mammary epithelial cells *in vivo* mediates STAT5 and p38 MAPK phosphorylation and promotes increased cellular survival, delayed involution, and latent tumor formation. Brk expression in human breast tumors may contribute to progression by inducing these same pathways, as evidenced in clinical samples of invasive breast carcinoma. Models of Brk expression in non-transformed mammary epithelial cells *in vitro* promote cellular survival in a context dependent manner, however, remain a strong tool for identifying molecules contributing to Brk mediated breast tumor progression. Inhibition of STAT5 and/or p38 MAPK may provide strong therapeutic potential in Brk-positive breast cancer.

TABLE OF CONTENTS

LIST OF FIGURES

Chapter 1

Chapter 3

Chapter 4

Chapter 5

LIST OF ABBREVIATIONS

Term	Abbreviation
Breast tumor kinase	Brk
Epidermal growth factor	EGF
Epidermal growth factor receptor	EGFR
Formalin fixed paraffin embedded	FFPE
Heregulin-β1	HRG
Hepatocyte growth factor	HGF
Human mammary epithelial cell	HMEC
Immunofluorescence	IF
Immunohistochemistry	IHC
Matrix metalloproteinase	MMP
Mitogen activated protein kinase	MAPK
Mouse mammary tumor virus	MMTV
(3-4,5-dimethylthiazol-2-yl)-2,5-diphenyltetrazolium bromide	MTT
Poly (2-hydroxyethyl methacrylate)	PolyHEMA
Prolactin	PRL
Prolactin receptor	PRLR
Protein tyrosine kinase	PTK
Receptor tyrosine kinase	RTK
Short hairpin RNA	shRNA
Src homology 2	SH2
Src homology 3	SH3
Signal transducer and activator of transcription	STAT
Terminal end bud	TEB
Whey acidic protein	WAP

CHAPTER 1

INTRODUCTION

According to the American Cancer Society, breast cancer accounted for 27% of newly diagnosed cancer cases in women in 2009, and an estimated 15% of cancer related deaths in women. As such a prevalent disease, the need to understand the cellular mechanisms of tumorigenesis is evident in an effort to both better understand and improve on current therapeutic approaches. Primary or acquired resistance to therapies is a common difficulty in treating breast cancer, therefore identifying and characterizing molecules that may play a role in resistance is a major focus of research today. In this dissertation, I will elaborate on experiments in which the modeling of breast tumor kinase/protein tyrosine kinase 6 in non-transformed mammary epithelium has identified novel signaling mechanisms that contribute to the pathogenesis of breast cancer.

PROTEIN TYROSINE KINASES

Protein tyrosine kinase (PTK) activity is elevated in breast cancer (2) and is associated with poor prognosis (3). PTKs are responsible for mediating several critical biological functions, such as cellular proliferation, migration, and differentiation (4-7). There are two types of PTKs: membrane spanning receptor tyrosine kinases (RTKs) and soluble, non-receptor tyrosine kinases that are not anchored to the cellular membrane.

RTKs activate intracellular signaling events via extracellular ligand binding. When a cognate growth factor binds to a receptor's extracellular ligand binding domain, receptor dimerization occurs. This dimerization in turn activates the kinase activity of the receptor, followed by transphosphorylation of the intracellular domains of the dimerized receptors. The phospho-tyrosine residues on the receptors are now recognized by the Src

homology 2 (SH2) domains of adaptor or scaffold proteins that also contain Src homology 3 (SH3) domains. These SH3 domains bind proline rich regions on downstream effector proteins to perpetuate phosphorylation mediated signaling events in the cytoplasm, which in turn activate or inhibit downstream effector proteins. After ligand-induced activation, signal termination can be obtained by the activity of tyrosine phosphatases directed towards the activated RTK or effectors, or by receptor endocytosis and degradation (6).

Non-receptor tyrosine kinases, or soluble PTKs, are activated in a similar manner to RTKs, however they do not bind ligand, and are located in the cellular cytoplasm, nucleus, or near the cell membrane. Each non-receptor tyrosine kinase consists of catalytic kinase domain, and an SH2 and SH3 domain.

BREAST TUMOR KINASE/PROTEIN TYROSINE KINASE 6

Breast tumor kinase/protein tyrosine kinase 6 (Brk/PTK6) is a non-receptor PTK whose cDNA was initially cloned in a screen for tyrosine kinases expressed in a

Figure 1.1: Brk Protein Domains

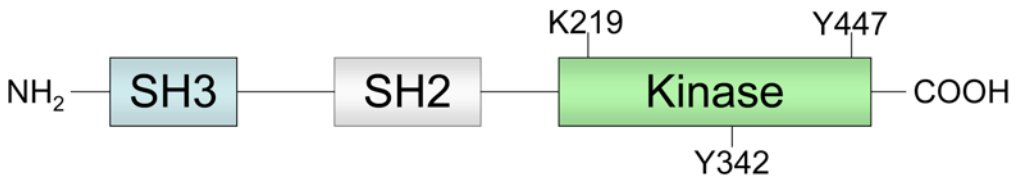

Figure 1.1. Brk protein domains and important regulatory residues. Brk protein structure consists of one N-terminal SH3 domain, one SH2 domain and a C-terminal kinase domain. Within the kinase domain are three resides important for Brk kinase activity. K219 is a lysine in the ATP binding pocket that is required for kinase activation. Mutation of this site to a methionine renders Brk kinase dead. Y342 is the tyrosine that is autophosphorylated upon kinase activation. Y447 is a tyrosine required for autoinhibition. Substitution of a phenylalanine at this site prevents results in a constitutively active Brk molecule.

metastatic breast tumor(8). The murine Brk ortholog Src-like intestinal kinase (Sik) was independently cloned from the small intestine and skin and has 80% identity to Brk (9, 10). Initially, a partial sequence for PTK6 was cloned from melanocytes (11). A distant relative of cSrc, the 451 amino acid Brk protein consists of an N-terminal SH2 domain, an SH3 domain and a C-terminal kinase domain that is subject to autophosphorylation and autoinhibition (12). However, unlike cSrc, Brk lacks an SH4 domain required for myristoylation, rendering it soluble. Similar to cSrc, Brk kinase activity is inhibited through interactions with its own SH2 and SH3 domains (12), but the Brk kinase domain shares higher homology to other family members (Srm, Frk and Src42A) than it does to the prototypical cSrc kinase domain (13).

BRK EXPRESSION IN TISSUES

Normal tissues that express Brk include the intestinal epithelium, melanocytes, keratinocytes (10, 11), the luminal epithelium of the prostate (14), and lymphocytes (15), however Brk is notably absent from normal mammary tissue (16).

Brk is expressed in up to 86% of invasive ductal breast carcinomas (1), as well as prostate and colon carcinomas (14, 16, 17), 70% of serous ovarian carcinomas(18), 37.5% of a small sample of head and neck squamous cell carcinoma (19), and a small percentage of metastatic melanomas (20). Whereas Brk expression in prostate cancer is detected in both well- and poorly-differentiated tumors (17), Brk expression levels increase in association with the histological grade of breast tumors (1) and invasiveness of breast cancer cell lines (21).

KNOWN BRK SUBSTRATES, PROTEIN INTERACTIONS, AND BIOLOGY

The list of Brk substrates and interacting proteins consists of proteins with varying functions. Of note are transcription factors signal transducer and activator of transcription (STAT) 3 and STAT5b, which are direct substrates of Brk, in vitro (22) (23), and critical regulators of mammary function (24, 25). Proliferation, migration and RNA binding are also regulated by Brk-mediated tyrosine phosphorylation of Sam68 (26), BKS/STAP-2 (27, 28), SLM-1 and -2 (29), paxillin (21), KAP3A (30), p190RhoGAP (31), and PSF (32). Most recently, Brk has been reported to directly phosphorylate beta-catenin (33) and Akt/pkB (34).

Proteins that can associate with Brk (shown by immunoprecipitation) include the RTKs EGFR/ErbB1, ErbB2, ErbB3 (35-37), adaptor proteins insulin receptor substrate-4 and GAP-A.p65 (38), and Erk5 MAPK (39)

Like other protein tyrosine kinases, Brk mediates a range of cellular processes related to the development or maintenance of malignancy. Brk expression sensitizes mammary epithelial cells to the mitogenic effects of EGF (35), and enhances PI3K signaling through increased ErbB3 phosphorylation (36) , therefore increasing the strength of potentially oncogenic signaling events. Cellular migration and invasion is regulated by Brk-mediated Rac1 activation and phosphorylation of paxillin in response to EGF treatment (21), and Brk-mediated p38 MAPK activity in response to heregulin treatment (1). Brk promotes anchorage independent growth when expressed in non-transformed mammary epithelial cells (35), and prevents detachment induced autophagic cell death in cancer cells (40), suggesting a potential mechanism for Brk-positive cancer

cells to survive the dissemination phase of metastasis. Brk also promotes proliferative Erk5 and p38 MAPK phosphorylation, as well as cyclin D1 expression in response to heregulin (1).

In non-transformed epithelial cells in vivo, Brk appears to play an inhibitory role in regards to cell proliferation. Studies with the PTK6 knock-out mouse illustrated Brk expression suppresses Akt mediated cellular proliferation in the intestinal crypts (41), via inhibiting beta-catenin mediated transcription (33). In keratinocytes, Brk mediates calcium induced terminal differentiation (38). Induction of Brk in the intestinal crypts sensitizes cells to DNA-damage induced apoptosis (42). However, when co-expressed in pluripotent Comma-1D murine mammary cells, Brk and ErbB2 act synergistically to decrease tumor latency in an orthotopic transplant model (37).

BRK AND THERAPEUTIC RESISTANCE

The role of Brk in de novo tumorigenesis is unknown, thus hypotheses about Brk-mediated tumorigenesis have come primarily from Brk-mediated events in breast cancer and breast cancer cell lines. It has been shown that the amplification of the chromosomal region that includes *brk* (20q13.3) is correlated with overexpression of the ErbB2 receptor, promoting proliferation in breast cancer (37). Brk can be implicated in resistance to therapies directed towards the EGF/ErbB receptor family because Brk is downstream of the RTKs being targeted (21, 35, 36). For instance, co-expression of Brk and ErbB2 in non-transformed MCF-10A cells results in decreased tumor latency and resistance to lapatinib (a dual kinase inhibitor targeting EGFR and ErbB2) treatment in a

mouse model (37). Previous work in the Lange lab has also shown constitutive Brk kinase activity in T47D breast cancer cells (which endogenously express Brk) and in MCF-10A cells (non-transformed mammary epithelial cells) stably transduced with an inducible Brk expression vector (1). These data suggest that Brk expression in non-transformed mammary epithelium (i.e. aberrant expression in a cell type that does not have endogenous Brk expression), does not rely on growth factor receptor activation to promote Brk kinase activity. However, in some cancer cell lines, Brk is sill responsive to growth factor treatment.

MURINE MAMMARY GLAND DEVELOPMENT

The mammary gland is a complex organ that undergoes dramatic changes in composition orchestrated by tightly regulated cellular events orchestrated by pituitary, ovarian and placental hormones. The mature mammary gland consists of an arborized network of epithelium embedded in the supporting stroma, or fat pad. Embryological mammary development begins on day 10 of gestation (E10) with the formation of the bilateral milk lines in the ventral epidermis of the embryo, which develop into five pairs of mammary buds by E14 (43). On E15.5 the mammary bud migrates further into the mesenchyme (led by active proliferation at the tip of the lengthening bud), eventually

Figure 1.2: Post-Natal Mammary Gland Development

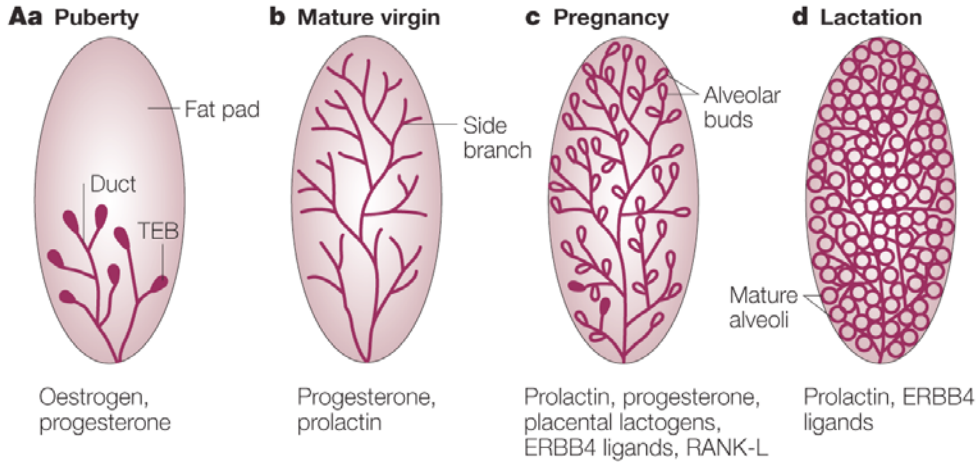

(Adapted from Hennighausen and Robinson, Nat. Rev. Mol. Cell Bio., 2005)

Figure 1.2. Post-natal mammary gland development and stage specific hormone/growth factor inputs. *A,* At puberty, cyclical production of estrogen and progesterone promotes ductal elongation and branching while the terminal end buds (TEB) proliferate and advance ductal growth through the fat pad. *B,* The mature virgin adult mammary gland is populated by a fully arborized ductal stucture. Side branches appear and disappear with cycling progesterone and prolactin levels. *C,* During pregnancy, elevated hormone levels drive alveolar budding and proliferation of secretory epithelium. *D,* Luminal epithelial cells produce and secrete milk into the lumen of mature alveoli during lactation.

developing into a rudimentary branched ductal tree by E18.5 (44).

The gland remains in this primitive state until puberty (fig. 1.2a), when the terminal end buds (TEB) respond to hormones and growth factors to lead the advancement and secondary branching of the ductal network further into the mammary fat pad (45). Cells trailing the TEB undergo programmed cell death, resulting in a network of hollow ducts (fig. 1.2b). Outside of fluctuations in secondary branching due to cycling hormonal cues during the estrous cycle, further functional differentiation is temporarily halted until pregnancy (46).

Pregnancy

Upon pregnancy, a marked increase in alveolar proliferation and differentiation occurs (fig. 1.2c), preparing the gland for lactogenesis. The expansion of the epithelial compartment during pregnancy is so extensive that, when fully developed, the gland appears to be composed of only epithelium. Adipocytes remain present, however, they are dramatically flattened, relatively undifferentiated, and much less abundant than in a mammary gland from any other developmental stage (47, 48). Once the suckling stimulus of the litter is discontinued, the process of glandular involution is initiated, which is responsible for returning the gland to a near virgin state.

Involution

When no longer needed, 50-80% of secretory mammary epithelium cells present in an active (lactating) mammary gland will undergo apoptosis and be removed in

preparation for the next pregnancy (49). Post-lactational involution is characterized by events that can be classified into two distinct stages. First, milk stasis (artificially induced by teat sealing) and the resulting mechanical strain increases pro-apoptotic Bax and Bcl-x_S expression in alveolar epithelial cells (50-52), as well as decreased circulating lactogenic hormone levels (53). Functional differentiation of the secretory epithelium is lost as a direct effect of the drop in prolactin-induced signal transducer and activator of transcription (STAT) 5 phosphorylation (24) and milk protein transcription (54). In the mouse, the first phase of involution can be halted if pups are reintroduced to a dam 48-72 hours after they were initially separated (55).

Whereas the first stage of involution related apoptosis is driven by events intrinsic to the mammary epithelium, the second stage of mammary involution (3+ days post-weaning) involves alterations in the stromal compartment as well. Protease mediated degradation and remodeling of the basement membrane and extracellular matrix (primarily via matrix metalloproteinase-2 (MMP-2), MMP-3, and MMP-9 produced by mammary stromal cells) promotes destruction of lobular structure and apoptosis in the mammary epithelium (56). As the epithelial content of the gland decreases, expansion of the adipocyte compartment occurs and continues until the gland resembles that of the virgin gland (57, 58).

The mechanism by which apoptotic mammary epithelial cells are removed from the mammary gland is not entirely understood. The presence of professional macrophages in the mammary gland has been detected at day 4 of involution (59). Macrophage recruitment to the involuting mammary gland is induced by the presence of

fibrillar collagen during the remodeling stage of involution (60), so the involvement of macrophages in the first stage of involution may be unlikely, but is yet to be determined. It has been suggested that mammary epithelial cells themselves may act as "amateur" macrophages by engulfing neighboring apoptotic mammary epithelium and prohibiting an inflammatory response (61, 62). Mammary epithelial cells express milk fat globule EGF factor 8 (MFG-E8) which facilitates binding and engulfing apoptotic cells displaying phosphatidylserine (63, 64), but it remains unknown whether this mechanism occurs at early involution timepoints.

MAMMARY INVOLUTION AND BREAST CANCER

In breast cancer, the presence of macrophages in tumors is associated with poor prognosis (65). Tissue remodeling during mammary involution has several molecular mechanisms in common with a wound healing response. For instance, Clarkson et al. (66) and Stein et al. (59) used microarray analysis to define gene expression profiles that strongly suggest an inflammatory component to early involution signaling (induced by forced weaning), including macrophage activation. Recent studies have illustrated that macrophages recruited during mammary gland involution are of those polarized to the potentially tumor promoting M2 phenotype as opposed to classical, tumor suppressive M1 macrophages (60, 67, 68). Understanding the parallels between involution related events in the normal mammary gland and oncogenic stimuli in breast cancer progression will benefit both areas of research.

MODELING MAMMARY CARCINOMA IN MICE

Although *in vitro* cell culture models are informative, the interactions between multiple cell types and structural components found *in vivo* are lacking, and there are concerns that cells used *in vitro* may not recapitulate their *in vivo* function or differentiation state. Historically, genetically engineered mice have been instrumental in characterizing oncogenesis in the complexity of the *in vivo* environment. Several genetically engineered mouse models of cancer develop mammary neoplasia, as a result of disrupting proper ductal and alveolar development or execution of glandular involution. With mammary function reliant on a series of tightly regulated proliferative and growth suppressive events, the dramatic cycles of glandular expansion and contraction introduce multiple opportunities for dysregulation that may result in oncogenesis. Whole animal genetic silencing (i.e. knockout) or transgenic overexpression of a molecule are basic approaches to assigning an *in vivo* function to proteins of interest. Tissue specific genetic modifications, however, are a more powerful tool, allowing more direct hypotheses to be challenged. Using promoters from genes with tissue specific expression patterns, transgene expression is limited a tissue compartment of interest. Transgene expression in the murine mammary gland is commonly achieved using the following promoters:

Mouse Mammary Tumor Virus (MMTV): Expression of the endogenous, retrovirally integrated MMTV in the mouse genome caused mammary tumors, and later led to the discovery of proviral activation of *Int1* (ortholog of *Wnt1*) and *Int2* (ortholog of *Fgf3*) in spontaneous tumors (69-72). Transgenic mice expressing an engineered fusion

protein of MMTV and myc developed mammary tumors, illustrating the tissue specific gene expression for the first time (73). Use of the MMTV promoter sequence drives transgene expression in all mammary epithelial cell types and results in detectable transgene expression at puberty, earlier than other commonly used mammary-specific promoters (74).

β-lactoglobulin (BLG): BLG is the major milk protein in most mammals, but is absent in rodent milk. Microinjection of a cloned sheep BLG gene into fertilized mouse eggs resulted in secretion of BLG by lactating mouse mammary glands. Hormonal regulation of BLG transgene expression was correctly interpreted despite no endogenous BLG gene in the mouse (75). BLG controlled transgenes are limited to expression in the secretory alveolar cells (74, 76).

Whey Acidic Protein (WAP): Hennighausen and Sippel cloned the cDNA sequence of WAP from mouse milk in 1982 (77). Circulating lactotrophic hormones induce expression of WAP in the mammary gland (78, 79). As WAP is a component of milk, maximal expression of endogenous WAP expression (and any genes subjected to control by the WAP promoter) occurs during late pregnancy and lactation in alveolar epithelium (80). WAP driven transgenes are inducible upon pregnancy, and as such are treated as inducible transgenic protein expression systems.

Phenotypic differences in the mammary gland may arise in mouse models of breast cancer as a consequence of promoter selection for transgene expression. For example, expressing a constitutively active form of TGF-β on an MMTV promoter results in a hypoplastic ductal network during development (81), but using the WAP

promoter, ductal morphogenesis is unaltered, and alveolar development and lactation is inhibited (82). Although each targeting strategy listed above is mammary specific, these differences can confound data interpretation when comparing models. However, this illustrates the theory that oncogenesis occurs via different mechanisms based on the context of temporal (puberty versus pregnancy/lactation) or the cellular subset (ductal versus alveolar) of oncogene/tumor suppressor expression.

CHAPTER 2

MATERIALS AND METHODS

CELL CULTURE

HMEC cells engineered to express a vector or Brk (described in (83)) cells were cultured in MEBM medium supplemented with a bullet kit (Lonza). HC11 cells were cultured in RPMI1640 (Gibco, Carlsbad, CA) supplemented with EGF, insulin, 5% FBS, and 1X penicillin/streptomycin. T47D cells were cultured in Minimum Essential Medium (MEM) (Gibco, Carlsbad, CA), supplemented with 5% FBS, 10μg/mL insulin, 1x non-essential amino acids (Cellgro), and 1x penicillin/streptomycin (Gibco). SKBR3 cells were cultured in McCoy's 5A medium supplemented with 10% FBS and 1x penicillin/streptomycin. MDA-MB-231 cells were cultured in Dulbeco's Modified Essential Medium (DMEM) (Gibco) supplemented with 10% FBS, 10μg/mL insulin and 1x penicillin/streptomycin. HaCaT cells were maintained in DMEM (Gibco) with 10% FBS and 1x penicillin/streptomycin added. All cells were cultured in a humidified incubator set at 37 degrees and 5% CO_2.

ANTIBODIES AND REAGENTS

WESTERN BLOTTING

Anti-Brk (sc1188) was purchased from Santa Cruz Biotechnology (Santa Cruz, CA). Antibodies specific for total and phospho-$Tyr^{694/699}$ STAT5, total and phospho-Thr^{180}/Tyr^{182} p38 MAPK were purchased from Cell Signaling (Danvers, MA). Anti-vinculin was purchased from Sigma (St. Louis, MO).

IMMUNOFLUORESCENCE

Brk (sc1188) was purchased from Santa Cruz. Laminin V antibody was a gift from the Yee lab. Alexa Fluor 488 and FITC labeled secondary antibodies, and ProLong Gold mounting medium with DAPI were purchased from Invitrogen (Carlsbad, CA).

IMMUNOHISTOCHEMISTRY

Brk (sc1188) was purchased from Santa Cruz Biotechnology. Phospho(Thr^{180}/Tyr^{182}) p38 MAPK (#4631), phospho(Tyr^{705})STAT3 (#9145?), phospho(Tyr$^{694/699}$)STAT5 (#9359), and cleaved caspase 3 (#9661) were purchased from Cell Signaling (Danvers, MA).

TREATMENTS

Purified, recombinant heregulin-β1 (HRG) was purchased from Upstate Biotechnology. Epidermal growth factor (EGF), prolactin (PRL) and doxorubicin (DOX) were purchased from Sigma Chemical (St. Louis, MO). Hepatocyte growth factor (HGF) was purchased from Millipore (Billerica, MA).

IMMUNOFLUORESCENCE AND CONFOCAL IMAGING

HaCaT and MDA-MB-231 were seeded at 50x10^5 cells/well on sterile 22x22mm glass cover slips (Gold Seal) in 6 well tissue culture dishes (Costar). Cells were serum starved for 48h, and treated with EGF, HGF or the appropriate vehicle controls. At the designated timepoints, medium and/or treatments were aspirated, the cells were washed with ice-cold PBS, and fixed with 4% formaldehyde.

PROLACTIN TREATMENT

HC11 murine mammary epithelial cells were plated and transfected with pCMV-3X-FL-Brk constructs using FuGene HD (Roche), serum starved 24h post-transfection, and treated with 500ng/mL prolactin (Sigma L6520). Cells were lysed using RIPA lysis buffer as previously described (84).

ANCHORAGE INDEPENDENCE

Six well dishes were coated with PolyHEMA (20mg/mL in 98% EtOH) and dried in an incubator overnight. Previously described HMEC+Brk cells (83) or HC11 cells transiently transfected (Roche FuGene HD) with Brk were plated 300K cells per well for 48hr. Cells in suspension were pelleted, trypsinized and stained with 0.4% trypan blue. Viable cells from each sample were counted in triplicate.

MAMMARY ORGANOID FORMATION

Eight-well chamber slides were coated with growth factor reduced Matrigel (BD Biosciences, Bedford, MA) as in (85) protocol paper. HMECs were then plated on the solidified Matrigel, allowed to adhere for 30 minutes in a 37° C incubator, and covered with medium containing 2% Matrigel. Every two days, the MEGM+2% Matrigel on top of the cultures was refreshed. After 8 days in culture, the assay medium was removed and cells were fixed and stained for immunofluorescent imaging.

CHEMORESISTANCE ASSAY

HMEC-vector and HMEC-Brk cells were plated in 24-well culture plates and allowed to adhere overnight. The next day, cells were treated with 0.1ng/mL, 0.5ng/mL or 1.0ng/mL doxorubicin in triplicate for 16 hours, after which cells were incubated with MTT dye for three hours, allowing metabolically active mitochondria to convert the yellow MTT into purple formazan crystals. DMSO:PBS (90%:10%) was added to solubilize the crystals, and the solution was subjected to spectrophotometry at 595nm as a indirect measure of cellular viability. Absorbance readings for the treatment groups were normalized to vehicle treated groups at the same timepoint.

TRANSGENIC MICE AND TISSUE PROCESSING

Transgenic mice expressing the human Brk (PTK6) gene under the control of the whey acidic protein (WAP) promoter were generated by microinjection of a WAP-Brk insert containing the wild-type Brk cDNA under the control of the WAP gene promoter (for expression in luminal mammary epithelial cells) into FVB/n embryos (University of MN Mouse Genetics Laboratory). The Brk cDNA was subcloned into the WKbpAII vector (a kind gift of Dr. Jeff Rosen, Baylor College of Medicine; (86)) using EcoR1 sites within the multiple cloning sequence. Two founders (one female, one male) were identified by PCR screening of tail biopsy DNA, and confirmed by Southern blotting (data not shown). Primer sequences for genotyping transgenic animals (by collection of DNA harvested from tail biopsies) span the Brk coding sequence (sense, 5'-agcgtgcacaagctgatgct-3') and the bovine growth hormone poly-A region of the transgene (antisense, 5'-

tctctggctgtctgtctgca-3'). Experiments were conducted under University of Minnesota IACUC approved protocols and NIH guidelines. All harvested tissues were fixed in 4% formaldehyde unless otherwise noted.

INVOLUTION TIMECOURSE

Virgin FVB/n or WAP-Brk mice were bred; litters were carried to term and normalized to 8 pups upon parturition. Pups were nursed for 10 days at which time the litter was force weaned. Mammary glands were harvested at 1 day post-weaning; involution day1 (INV1), INV4, INV6, INV9, and INV14.

WHOLE MOUNTS

Inguinal mammary glands were harvested and fixed, washed with PBS and stained with Carmine Alum (2g/L Carmine and 5g/L aluminum potassium sulfate [Sigma C-1022 and A-7167, respectively] in ddH_2O). Glands were then dehydrated in graded ethanols, cleared with xylenes, and affixed to slides.

IMMUNOHISTOCHEMISTRY AND DIFFERENTIAL STAINS

A Leica 1020 automated processor was used to process tissues through graded alcohols (70%-100%) and CitriSolv washes before being paraffinized. Tissues were further incubated in an oven under vacuum for 1h in molten paraffin then embedded. Three- to five-micron thick sections were cut and mounted on Fisher Superfrost/Plus slides.

IMAGING AND ANALYSIS

Digital images were taken of three fields per gland at 200X or 400X total magnification. For epithelial content determination, a grid of 360 boxes was overlaid on 200X images and boxes containing epithelial cells were counted. For IHC quantification, NIH ImageJ (Rasband, W.S., ImageJ, U. S. National Institutes of Health, Bethesda, Maryland, USA, http://rsb.info.nih.gov/ij/, 1997-2009.) was used with a cell counter plug-in to manually count positively stained mammary epithelial cells vs. total epithelial cells in multiple fields. Annotated regions were drawn on each digital H&E image using a pen tablet (Intuos3, Wacom, Kazo-shi, Saitama, Japan) for area calculations by determining epithelial pixel count relative to the entire gland, and selecting regions of interest for digital IHC analysis. For digital IHC quantification, slides were scanned at 40x magnification (0.25microns/pixel) using a whole slide scanner (ScanScope CS, Aperio Technologies, Vista, CA) fitted with a20x/0.75 Plan Apo objective lens (Olympus, Center Valley, PA). Images were saved in SVS format (Aperio) compressed with JPG2000 at 70% quality. Images were saved on a server and retrieved using whole slide image management software (Spectrum, Aperio).

Five annotated regions were drawn on each slide using a pen tablet screen (Cintiq 21UX, Wacom, Kazo-shi, Saitama, Japan) on the whole slide images viewed at high resolution using the Aperio system's annotation software (ImageScope 10, Aperio).

A nuclear cell quantification image analysis algorithm (IHC Nuclear Quantification, Aperio) was trained on control slides by defining the color vectors for the hematoxylin nuclear counterstain and primary positive chromagen DAB, minimum and maximum size for nuclei, and threshold ranges for intensity of nuclear staining. The analysis algorithm was trained to detect nuclei in four intensity ranges for cells with no positive staining, weak positive staining, medium positive staining, and strong positive staining. The analysis was performed on each annotated region using the defined settings and the nuclear count results were collected from each slide. The data were represented as an H-score (87), which accounts for staining intensity and percentage of positively stained cells. The H-score = (% of 0 intensity staining nuclei*0) + (% of 1 intensity staining nuclei)*1 + (% of 2 intensity staining nuclei) *2 + (% of 3 intensity staining nuclei) *3.

MAMMARY EPITHELIAL CELL ENRICHMENT

Mammary glands at various developmental stages were harvested and weighed. After manual disruption with no. 21 scalpels, the homogenate was incubated for 3h in a 37º C in 4mL digestion buffer (Ham's F12/DMEM [BioWhitaker 12-719F] plus 2mg/mL collagenase A [Roche 11088785103] and 100U/ml hyaluronidase [Sigma H3506]) per gram of tissue. Digested mammary glands were centrifuged and washed with Ham's F12/DMEM+1% serum three times at 1500 rpm, then twice at 800 rpm. The resulting cell pellets were lysed in RIPA lysis buffer and subjected to Western blotting as in (84)with the addition of Roche PhosStop and Complete inhibitor tablets.

IMMUNOHISTOCHEMISTRY

Formalin fixed, paraffin embedded sections of mammary glands were deparaffinized and rehydrated through xylene and graded ethanol washes. Sections were equilibrated in PBS and microwaved in antigen retrieval buffer (10mM Sodium Citrate, pH 6.0 for 20 minutes or 1mM EDTA, pH 8.0 for 10 minutes). Slides were washed with ddH_2O then PBS and placed in 3% H_2O_2 for 10 minutes to block endogenous peroxidases. Sections blocked with serum-free protein block (Dako X0909) were incubated overnight at 4º C with primary antibodies diluted in Dako Antibody diluent (S0809), washed with PBST and incubated in biotinylated secondary antibody (Vectastain Elite Kit, PK-101) for 30 minutes at room temperature. Slides were washed, then incubated with Vectastain Elite RTU ABC reagent (PK-7100) and subjected to colorimetric detection with ImmPACT DAB substrate (Vector, SK-4105). Antibodies: Brk (sc1188) was purchased from Santa Cruz. Phospho-p38 MAPK (#4631), phospho-STAT3 (#9145), phospho-STAT5 (#9359), and cleaved caspase 3 (#9661) were purchased from Cell Signaling.

PROLACTIN TREATMENT

HC11 murine mammary epithelial cells were plated and transfected with pCMV-3X-FL-Brk constructs using FuGene HD (Roche), serum starved 24h post-transfection, and treated with 500ng/mL prolactin (Sigma L6520). Cells were lysed using RIPA lysis buffer as previously described (84). Immunoblotting was performed with Brk (Santa Cruz #1188, and an in-house antibody #746), total STAT5 (Cell Signaling #9363), p-

STAT5 (Cell Signaling, #9145), total p38 MAPK (Cell Signaling #9212), p-p38 (Cell Signaling #4631, #9211), and anti-vinculin (Sigma #V9131).

ANCHORAGE INDEPENDENCE ASSAY

Six well dishes were coated with PolyHEMA (20mg/mL in 98% ethanol) and dried in an incubator overnight. Previously described HMEC-Vector and HMEC-Brk cells (83), or HC11 cells transiently transfected (Roche FuGene HD) with Brk were plated 300K cells per well for 48hr. Cells in suspension were pelleted, trypsinized and stained with 0.4% Trypan Blue. Viable cells from each sample were counted in triplicate in three independent assays.

TISSUE MICROARRAY

A series of human breast tissue samples surgically obtained from healthy women undergoing reduction mammoplasty (n=23), or with pathological conditions that included fibroadenoma (n=22), infiltrating ductal carcinoma (n=23) and infiltrating lobular carcinoma (n=23) were made available as FFPE archival material from the Department of Pathology, Third Medical Faculty in Prague, Czech Republic. The original slides were re-evaluated by a pathologist (Dr. Daniel Housa) to confirm the initial pathology diagnosis, and representative slides were selected for further processing.

Tissue microarrays were constructed from routinely prepared formalin fixed, paraffin embedded tissue blocks in parallel, using a manual tissue arrayer TA1 (A Fintajsl, Czech

Republic). The representative area of interest was selected on the original glass slide and corresponding area on donor tissue block was inked. Tissue cylinders, 1.6 mm in diameter, were punched from the marked regions of each donor tissue block, and transferred to a recipient block for the array. One hematoxylin and eosin section was made from each block to ensure the presence of tumor regions. Scoring of positively stained regions was performed by arbitrary establishment of a threshold for positive IHC staining intensity. The scores consist of 0= no staining relative to no primary controls, 1= weak diffuse staining, 2= moderate diffuse staining, 3= strong diffuse staining. Any focal staining present increased the score by 1 (i.e. a weakly diffuse stain with regions of strong focal staining was scored a 2). Only the adenoma or carcinoma compartment was scored, except in the reduction mammoplasty group, where the entire section was analyzed.

STATISTICS

Unless otherwise noted, all results are presented as means +/- SEM. Paired t-tests were done with statistical significance occurring when $p \leq 0.05$.

CHAPTER 3

INDUCIBLE, TISSUE SPECIFIC EXPRESSION OF BRK/PTK6 DELAYS MAMMARY INVOLUTION AND PROMOTES TUMORIGENESIS

INTRODUCTION

Protein tyrosine kinase (PTK) activity is elevated in breast cancer (2) and is associated with poor prognosis (3). PTKs and their downstream signaling pathways contribute to critical biological functions relevant to the cancerous phenotype, such as increased cellular proliferation, pro-survival, invasion and migration/metastasis. One such cancer-associated PTK is breast tumor kinase/protein tyrosine kinase 6 (Brk/PTK6). Brk was cloned in a screen for tyrosine kinases expressed in a metastatic breast tumor (8). The murine Brk-ortholog, Src-like intestinal kinase (Sik), was independently cloned from the small intestine and skin and shares 80% identity with Brk (10). A distant relative to c-Src, Brk shares a similar domain structure, consisting of an N-terminal SH2 domain, an SH3 domain, and a C-terminal kinase domain that is subject to autophosphorylation and autoinhibition (12)However, the Brk C-terminus lacks a motif required for myristoylation (i.e. as found in c-Src), rendering it truly "soluble" or mobile within and between cellular compartments (8, 10).

Brk is overexpressed in up to 86% of invasive ductal breast carcinomas (1, 88), prostate and colon carcinomas (14, 16, 17), 70% of serous ovarian carcinomas (18), 37.5% of a limited sampling of head and neck squamous cell carcinomas (19), and a small percentage of metastatic melanomas (20). Increased Brk expression levels are associated with the carcinoma content of breast tumors (1), tumor grade (40), and invasiveness of breast cancer cell lines (21). Normal tissues that express Brk include the intestinal epithelium, melanocytes, keratinocytes (10, 11), prostate luminal epithelium (14), and lymphocytes(15). However, Brk is notably absent from normal mammary

tissue (16). The list of known Brk substrates and interacting proteins is limited, but consists largely of signaling or signal transduction-related adaptor molecules, and RNA- or DNA-binding proteins, including signal transducers and activators of transcription (STATs). Notably, both STAT3 and STAT5b have been shown to be direct substrates of Brk *in vitro* (22, 23). These molecules are also required regulators of mammary gland lactogenic differentiation (STAT5,(24)) and regression (STAT3, (89)).

Mammary gland development is a highly dynamic and hormonally-driven process; in mammals, functional glands are not fully mature until early adulthood/pregnancy. Beginning as an invagination of dermal epithelium in the embryo, the mammary anlage migrates into the mesenchyme, eventually elongating into a rudimentary branched ductal tree (44). The gland remains in this primitive state until puberty, when the terminal end buds (TEBs) respond to hormonal cues and lead the advancement and secondary branching of the ductal network further into the mammary fat pad resulting in a network of hollow ducts. Outside of fluctuations in secondary branching due to cycling hormonal cues during the estrous cycle (46), further functional differentiation is temporarily halted until pregnancy. Upon pregnancy, a marked increase in ductal branching and alveolar proliferation and differentiation occurs, preparing the gland for lactogenesis. While pups are feeding, the mammary gland remains in the differentiated state due to the continued presence of lactogenic hormones such as prolactin and growth hormone (53).

Once the suckling stimulus of the offspring is removed, involution is initiated. In mouse models, completion of this regressive 10-day process returns the gland to a near

virgin state. Post-lactational involution is characterized by events that can be classified into two distinct stages. First, milk stasis and the resulting mechanical stresses initiate a tightly regulated wave of apoptosis in alveolar epithelial cells (and their concomitant removal) (50, 51), followed by the second stage in which remodeling of the ECM and the expansion of the stromal adipocyte compartment occurs (57, 58).

Mouse models have been extensively used to understand genetic mechanisms of breast cancer biology (90-92). Classical models of human breast oncogene overexpression in the mouse mammary gland demonstrate altered biological processes responsible for proper ductal and alveolar development, as well as modified initiation and execution of glandular involution (Examples: active MMTV-Akt (93), WAP-Bcl2 (94), MMTV-EGFR (95), MMTV-ErbB2/neu (96)). Modeling human tumorigenesis in the murine mammary gland is a valuable approach for investigating oncogene mediated biology, as the dynamic nature of the mammary gland *in vivo* (with regards to hormonal cues and cellular heterogeneity) more closely mimics the human breast than cells cultured *in vitro*.

In this study, we describe the first transgenic model of mammary gland specific (i.e. WAP-promoter-driven) Brk expression. Using newly created WAP-Brk transgenic mice, we studied the physiological process of mammary gland involution to investigate the impact of Brk expression on the survival of mammary luminal epithelium, and altered regulation of pro-survival signaling pathways that may be permissive for mammary tumorigenesis.

RESULTS

WAP-Brk transgene is expressed in the mammary gland

To determine the effects of Brk expression in the normal mammary environment *in vivo*, Brk cDNA was placed under the control of the WAP promoter (fig. 3.1a), which directs transgene expression predominantly to the luminal epithelium upon lactation. (80). Four founders were generated by pronuclear injection of the linearized transgene. Two mice successfully bred to establish independent lines, with transgene presence being verified by PCR (fig. 3.1b) (which were later denoted as Brk^{low} or Brk^{high} upon their protein expression). Transgene expression in whole cell lysates of mammary epithelial enrichment preparations from females was determined by Western blot with a Brk specific antibody. After induction of milk protein synthesis, Brk protein expression was not detected in virgin or pregnant mice as expected, but was detected during the process of mammary involution (fig. 3.1c) beginning 1 day after pup removal and continuing through at least 6 days post weaning. Total STAT3 levels were lower in MEC purified from mammary glands of pregnant relative to virgin animals, but remained relatively constant during involution days 1-6. Interestingly, however, the band representing STAT3 was upshifted (i.e. phosphorylated) in lysates from wild-type but not transgenic mice (involution days 4-6). These data suggest that forced expression of Brk may alter the time course of mammary involution, as measured by regulation of phospho-STAT3 (fig. 3.1c). Immunohistochemistry on formalin fixed paraffin embedded (FFPE) tissues also detected significant Brk expression in both lines (fig. 3.1d), with the 11097/Brk^{high}

line exhibiting a higher level of Brk. Brk protein was undetectable in wild-type controls by both protein detection methods.

Fig. 3.1: WAP-Brk transgene and expression

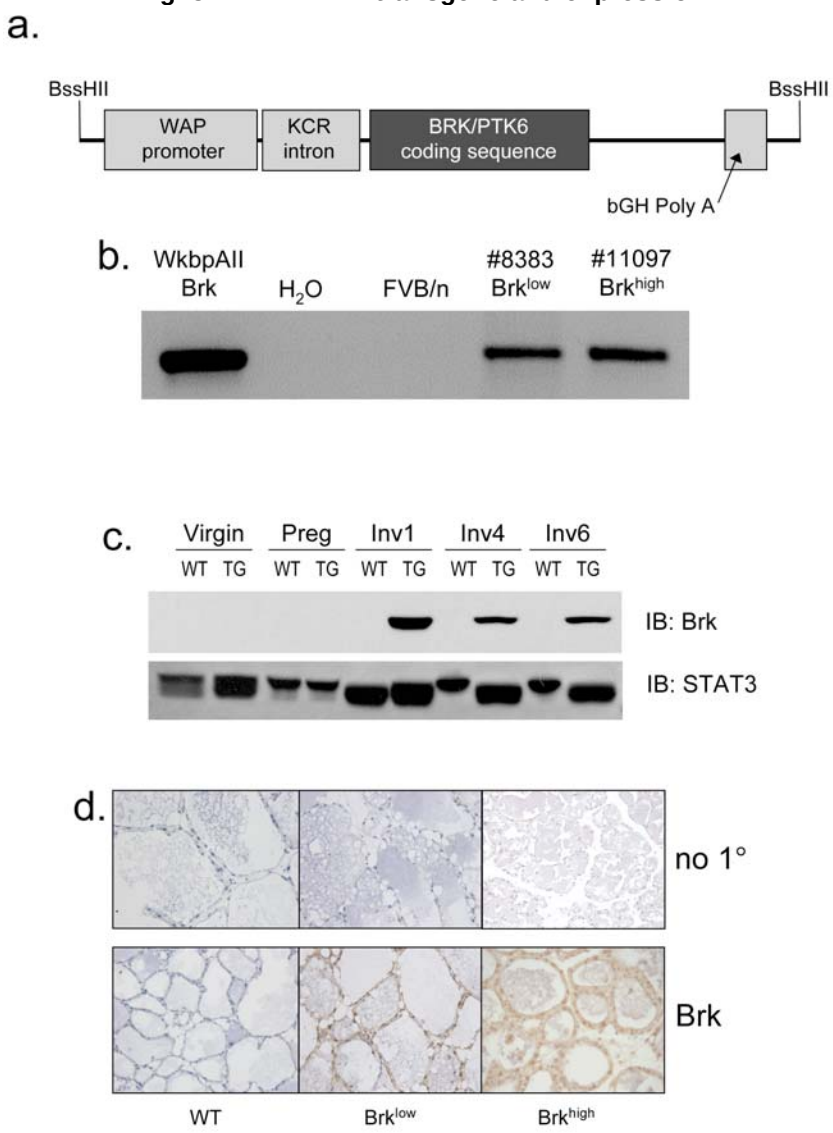

Figure 3.1. Transgene, screening and expression. *A*, transgene structure, including WAP promoter, beta-globin intron to enhance Tg expression, Brk/PTK6 coding sequence, and growth hormone poly A signal. Tg was linearized with BssHII digestion. *B*, PCR screening of founder mice and controls. (*L-R*: purified construct, water, wild-type FVB, and two WAP-Brk founders.) *C*, Whole cell lysates from wild-type and Brk^{high} mammary glands were subjected to Western blotting for Brk, after enrichment for epithelial cells from virgin, pregnant, and involuting (days 1, 4 and 6 post-weaning) glands. 75ug protein loaded. *D*, Brk IHC in FFPE mammary gland sections. Inguinal glands shown are from INV1. Positive staining is indicated by brown precipitate.

WAP-Brk expression alters the kinetics of mammary involution

We investigated whether Brk expression in the mammary gland resulted in proliferative or inhibitory effects on the mammary epithelium. We hypothesized there would be a proliferative or pro-survival phenotype, similar to studies that have expressed other oncogenes in the mammary gland (93, 97). Initially, no noticeable differences in pup size or development were seen between wild-type or transgenic mice, indicating the lack of a developmental or differentiation related phenotype (data not shown). Evidence of hyperproliferative defects in mammary development were not visible when whole mounts of pregnant or lactating mammary glands were evaluated, however upon analysis of mammary glands undergoing involution, it was noted that mammary glands from Brk transgenic mice were slightly larger and had a higher cellular content than their wild-type counterparts (fig. 3.2a). Hematoxylin and eosin staining of mammary sections revealed a lag in remodeling of Brk glands versus wild-type glands at the same stage of involution (fig. 3.2b). Alveoli at day 1 (D1) of involution showed no difference in development or milk content, however Brk glands appeared to have less apoptotic epithelial cells being shed into the lumen. Shedding alveolar cells are present in the lumen on day 4 (D4) of involution in transgenic glands whereas there are none present in wild-type glands, and there are larger clusters of secretory alveoli, compared to wild-type glands. By day 6 (D6), mammary glands from wild-type and Brk mice were mostly repopulated with adipocytes, but glands from Brk mice still exhibited functional alveoli, as indicated by the noticeable presence of milk. Days 9 (D9) and 14 (D14) of involution appeared similar in both wild-type and transgenic lines.

Fig. 3.2: WAP-Brk delays mammary involution

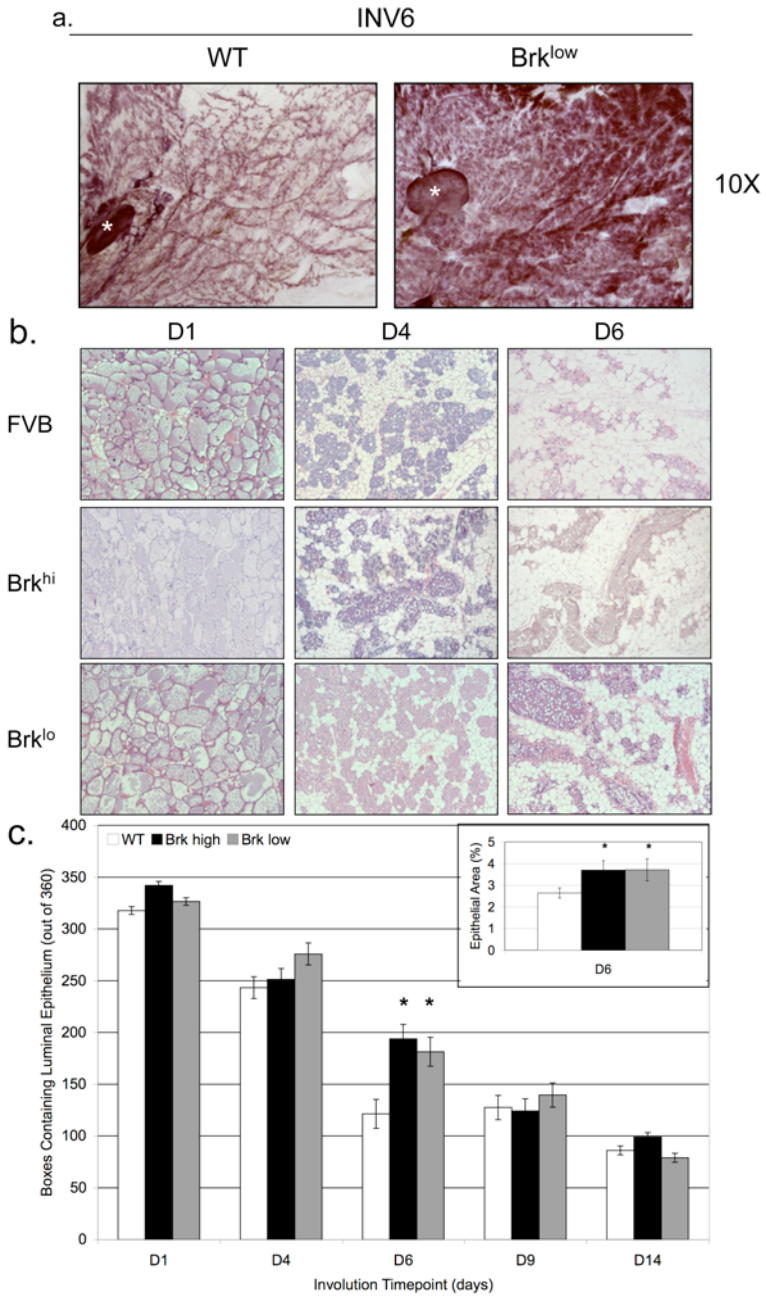

Figure 3.2. WAP-Brk mammary glands exhibit delayed post-lactational involution. *A*, Carmine alum staining of inguinal mammary gland whole mounts, involution day 6. (*Left*: WT, *Right*: Brk^{low}) *B*, H&E staining of involuting mammary glands from 1-6 days post weaning. 200X original magnification. *C*, Quantification of mammary epithelium from H&E sections. *Inset*, epithelial content quantified by area on day 6. *=p<0.05

In order to quantify the epithelial content of mammary glands from wt or Brk transgenic mice, digital images of H&E sections were analyzed. Using an arbitrary grid of 360 boxes overlaid onto an image, the presence or absence of luminal epithelial cells was recorded, and presented as a fraction of the total grid (fig. 3.2c). Epithelial cell content did not differ during early (days 1-3) involution. However, beginning with day 4 and significantly at day 6, glands from Brk transgenic animals presented with higher epithelial content relative to same day wild-type glands; these differences were resolved by day 9. To validate our analysis using the grid method, the epithelial cell area was re-calculated by selecting epithelial regions of mammary tissue, determining the area of the selected regions (in pixels), and presented as a fraction of the whole gland at day 6 (inset, fig. 3.2c). In this analysis, Brk^{high} transgenic mice demonstrated a statistically significant increase in epithelial area when compared to day 6 wild-type glands (3.6% versus 2.5%, $p<0.05$, $n=3$). These data suggest that Brk expression induces a delay or lag in mammary gland involution, most apparent between days 4 and 6 of forced involution; transgenic glands recover this difference by days 9-14.

WAP-Brk Mice Exhibit Decreased Involution-Related Signaling

To further confirm a Brk-induced delay in mammary gland involution (fig. 3.3), we investigated signaling inputs associated with early initiation and execution of involution. The first stage of involution (approximately 3 days post pup removal) is characterized by massive apoptosis and luminal shedding of epithelial cell bodies formerly lining the ducts (98). To detect luminal epithelial cells undergoing apoptosis in

mammary glands from wild-type or Brk mice, IHC was performed with antibodies directed against cleaved caspase 3, a mediator of apoptosis(99). Multiple representative images (fig. 3.3a, images) were scored for positive cells, with visible dead cells already shed into the lumen also being counted as positive. Data were quantified by counting both the number of IHC positive and negative cells. At day 4 of involution, less caspase 3 cleavage occurred in mammary glands from WAP-Brk mice relative to wild-type control glands (fig. 3.3a, bar graph). By day 6 of involution, apoptotic cell numbers had reached similar levels in glands from Brk transgenic and wild-type type animals.

STAT3 is a critical mediator of the induction of involution (25, 89); expression of STAT3 is required for mammary involution, and its phosphorylation is induced at the beginning of involution and gradually decreases (25, 50, 89). Our protein expression studies (Fig. 3.1c) suggested altered (i.e. suppressed) STAT3 phosphorylation in Brk transgenic glands relative to wt controls. To directly measure STAT3 phosphorylation in our Brk transgenic model, IHC was performed on wt and Brk-expressing mammary glands during the involution time course. Representative fields (fig 3b, images) from each time point were scored for the presence or absence of p-STAT3 staining in individual cells of the luminal epithelium, and presented as a percentage of total cell count. The levels of STAT3 phosphorylation were similar in all lines at involution days 1 and 14. However, at days 4 and 6, mammary glands from Brk transgenic mice exhibited roughly 10-20% less p-STAT3 relative to those from wild-type-type mice (fig. 3.3b, bar graph). In glands from WAP-Brk mice, the levels of phospho-STAT3 decreased precipitously

from day 1 to 4, compared to the wild-type type mice, in which the decrease was not evident until day 9. Similar to the epithelial content (fig 3.2), STAT3 signaling in transgenic vs. wild-type-type mice returns to comparable levels after day 9, resulting in an approximate 20% basal level of STAT3 phosphorylation in resting or fully regressed glands. Taken together, these data support a Brk-dependent delay of early involution, as indicated by fewer apoptotic cells (day 4) and transient suppression of STAT3 phosphorylation (days 4-6), an independent marker of involution induction.

Fig. 3.3: Decreased involution signaling in WAP-Brk glands

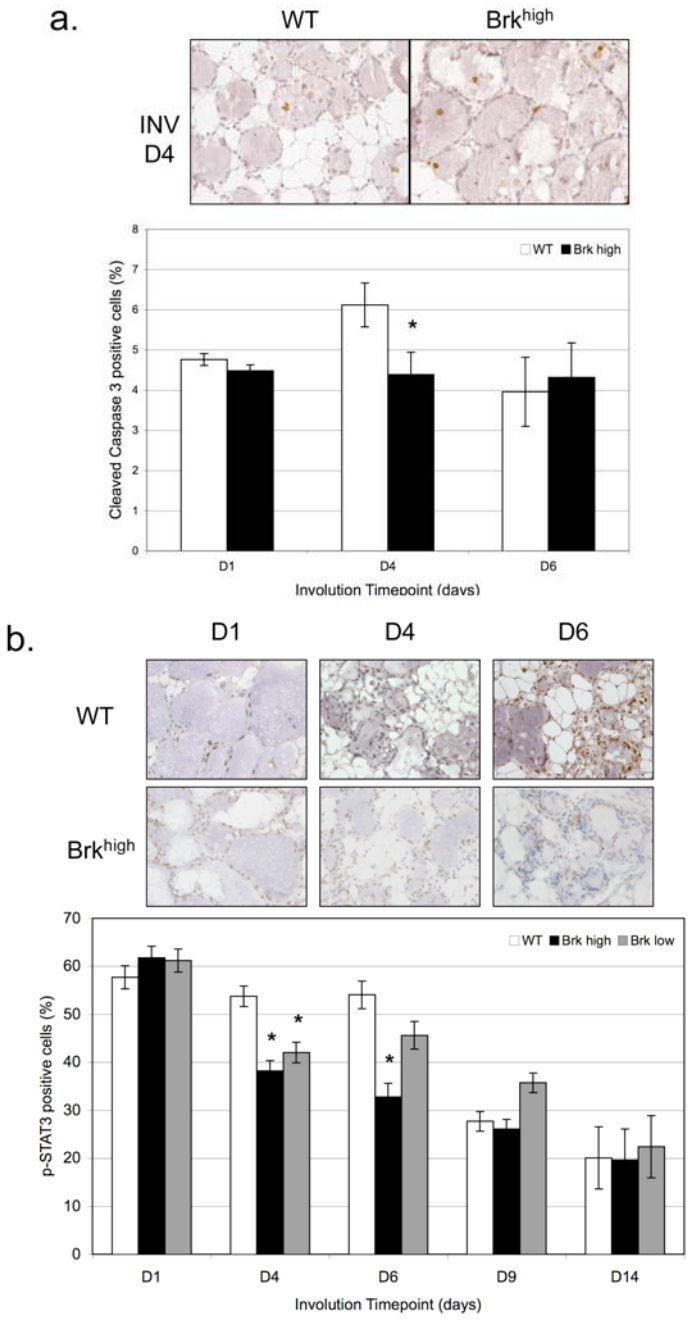

Figure 3.3. Involution signaling is decreased in WAP-Brk mice. *A*, IHC for cleaved caspase 3. *Images*: representative images of day 4 of involution (INV D4) in wild-type and Brk^{high} mice. 400X original magnification. *Graph*: Quantification of positive IHC staining, presented as a percentage of total mammary epithelium. *B*, IHC for STAT3 (pY705) in involuting glands. *Images*: Representative images of p-STAT3 IHC, involution days 1-6 (INV1-INV6). 400X original magnfication. *Graph*: Quantification of positive IHC staining, presented as a percentage of total mammary epithelium.

Brk Expression Promotes Increased Phosphorylation of STAT5 and p38 MAPK

To link potential Brk-dependent signaling events to alterations in the time course of mammary gland involution, we investigated the phosphorylation status of STAT5, an *in vitro* Brk substrate (23) and critical regulator of mammary gland differentiation (24, 100). STAT5 is phosphorylated and activated in response to prolactin signaling during the massive epithelial expansion that takes place during alveolar development (24, 101, 102). STAT5 is relatively under-studied during mammary involution. However, inverse to STAT3, levels of phospho-STAT5 are reported to be high during early mammary involution (~day 1), but then precipitously drop over a 2-6 day period (24, 25). Following a time course of involution, sections of FFPE mammary glands were harvested from either wild-type-type or WAP-Brk mice and evaluated by IHC using phospho-specific STAT5 antibodies (fig. 3.4a, images). Upon initial inspection, p-STAT5 staining appeared to be more intense in glands (INV4-6) from WAP-Brk mice relative to wild-type controls. Phospho-STAT5 stained images were quantified by digital analysis (as described in Methods) and represented as an averaged H-score. Surprisingly, this analysis revealed that at day 4, STAT5 phosphorylation is actually higher in mammary glands from wild-type mice relative to WAP-Brk mice. Consistent with previous studies (24), p-STAT5 levels dropped (to a score of near 0) at day 6 in glands from wt mice, reflecting the relative lack of p-STAT5 at this time point (fig 3.4a, graph). In contrast, WAP-Brk mice contained measurable (H score of ~6) pSTAT5 levels at day 6, a time point when cellular content also differs the most between glands of wild-type and Brk mice (fig. 3.4). Proportionally, glands from wild-type mice underwent a 47-fold drop in pSTAT5 levels

Fig. 3.4 Brk promotes phosphorylation of STAT5 and p38 MAPK

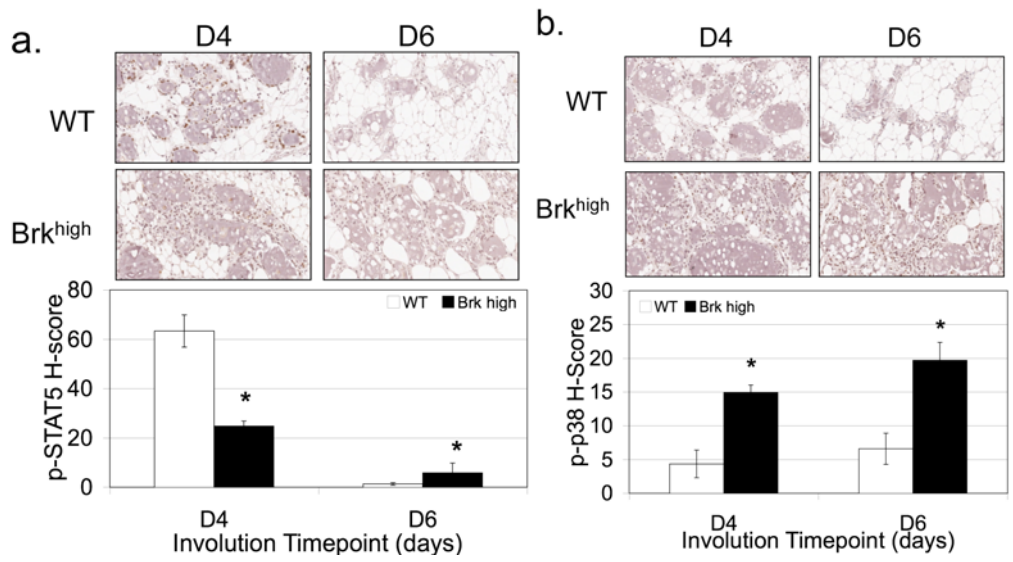

Figure 3.4. Brk promotes STAT5 and p38 MAPK activation in mammary epithelium. *A*, WAP-Brk expression increases STAT5 phosphorylation at Y694 in mammary glands. *Images*: Representative p-STAT5 IHC in involuting mammary glands, INV D4-D6. *Graph*: Quantification of p-STAT5 positive IHC, presented as an H-score (see Methods). *B*, WAP-Brk mammary glands exhibit increased p-p38 MAPK. *Images*: representative IHC staining p38 MAPK(pT180/Y182) from sections of inguinal mammary glands from INV D4-D9. 400X original magnification. *Graph*: Quantification of p-p38 MAPK positive IHC. Data presented as an H-score. *p=<0.05, n=3 glands, 5 regions analyzed per gland.

(H-score), relative to only 4.3-fold in glands of WAP-Brk mice. These results suggest that although the degree of STAT5 phosphorylation is lower in Brk transgenic mice at day 4, prolonged duration of the p-STAT5 signal (significantly higher at day 6 in Brk mice) may contribute to delayed involution primarily observed (fig 3.2) at this time point (day 6).

Previously, we reported that Brk promotes increased breast cancer cell proliferation and migration in response to the erbB ligands, EGF and heregulin, in part via Brk-dependent signaling to p38 MAPK (1). Although early studies initially described p38 MAPK as a mediator of stress responses and linked to activation of apoptosis

pathways in multiple tissues, this kinase is closely associated with pro-survival phenotypes in the context of breast cancer (103). We predicted that Brk-transgene expression in the mammary gland may increase p38 MAPK activity, perhaps leading to prolonged luminal epithelial cell survival and delayed involution (fig. 3.2). FFPE sections from involuting mammary glands were processed for phospho-p38 MAPK IHC (fig. 3.4b, images), digitally analyzed and again assigned H-scores (as above) data represent the degree of p38 MAPK positivity and staining intensity (fig. 3.4b, bar graph). Notably, at both days 4 and 6 of involution, we detected an approximately 3-fold increase in the H-scores of glands from Brk transgenic mice relative to glands from same-day wild-type mice. Both the number of cells staining for phospho-p38 and the intensity of staining (per cell) were increased. These data suggest that in the context of mammary gland involution, p38 MAPK acts as a pro-survival signal.

PRL Induced STAT5 and p38 MAPK Phosphorylation in HC11 Cells is Increased by Exogenous Brk Expression

HC11 cells are a spontaneously immortalized subclone of the Comma1D cell line, which was isolated from a BALB/C mouse mammary gland during mid-pregnancy (104, 105). As a result of the intermediate developmental stage of the cells, functional differentiation is possible *in vitro* (106). As such, HC11 cells have become a valuable commodity for investigating mammary gland biology in a non-transformed cell model, because they represent a functionally normal mammary epithelial cell that responds to lactogenic hormones and growth factors such as prolactin and growth hormone. At the

protein level, HC11 cells do not express Sik (the murine ortholog of Brk) making them an excellent cell-based model of non-transformed mammary epithelium for Brk overexpression studies. Brk does not play a role in embryonic mammary development, as the Sik knockout mouse had no mammary phenotype (41), however it is possible that Brk exerts its proto-oncogenic effects on the mammary gland during the process of functional differentiation. To mimic aberrant expression of Brk in the context of non-transformed, partially differentiated mammary epithelium, we transfected wild-type Brk into the HC11 cell line, and investigated cellular signaling in response to the physiological relevant ligand, prolactin.

Cells were transiently transfected with Brk, and serum starved prior to PRL treatment. Western blotting revealed that 500ng/mL PRL induces robust phosphorylation of STAT5. In HC11+Brk cells, both the intensity and kinetics of STAT5 phosphorylation are altered relative to HC11+vector cells, with the HC11+Brk cells showing overall increased STAT5 phosphorylation, and an earlier post-treatment activation (fig 3.5a).

Transiently expressing exogenous Brk in HC11 cells also resulted in an increase in basal p38 MAPK phosphorylation in the absence of growth factors and hormones. In addition, treatment with prolactin also induced phosphorylation of p38 in a time dependent manner, with altered kinetics in HC11+Brk cells (fig. 3.5b).

Fig. 3.5: Brk promotes Prolactin induced STAT5 and p38 MAPK Activation

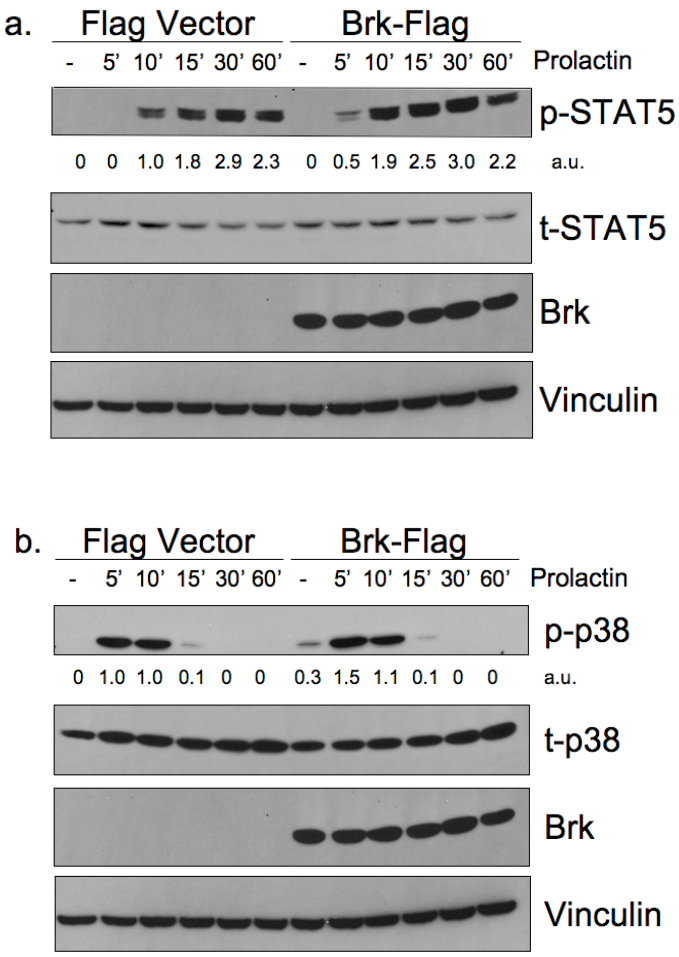

Figure 3.5: Brk expression sensitizes HC11 cells to prolactin treatment. HC11 murine mammary epithelial cells were transiently transfected with pCMV-3X-Flag (Flag Vector) or pCMV-3X-Flag-Brk (Brk-Flag), followed by serum starvation and prolactin treatment (500ng/mL) for 5, 10, 15, 30, or 60 minutes. Cells were lysed and subjected to SDS-PAGE and Western blotting. Densitometry was performed on the phospho-blots, normalized to the corresponding total protein control blot, and represented as arbitrary units (a.u.). *A*, Phospho-STAT5 (p-STAT5) blot, with signal intensity normalized to total STAT5 (t-STAT5). *B*. Phospho-p38 MAPK (p-p38) blot, with signal intensity normalized to total p38 MAPK (t-p38).

Brk induces anchorage independent survival

A critical step in tumorigenesis is the loss of contact inhibition and anchorage dependent survival. Non-transformed epithelial cells require contact with the basement membrane to perform their function as a barrier to the outside surface of the body. Recent studies have shown that Brk expression promotes anchorage independent survival (40, 107). Using previously engineered HMEC-Brk cells (83)or HC11 cells transiently transfected with Brk, we investigated the effect Brk would have in our models for Brk expression in non-transformed mammary epithelial cells.

HMEC-vector, HMEC-Brk, HC11-vector, and HC11-Brk cells were plated in six-well culture dishes coated with PolyHEMA, a polymer that prohibits cell attachment to

Fig. 3.6: Brk Promotes Anchorage Independent Survival

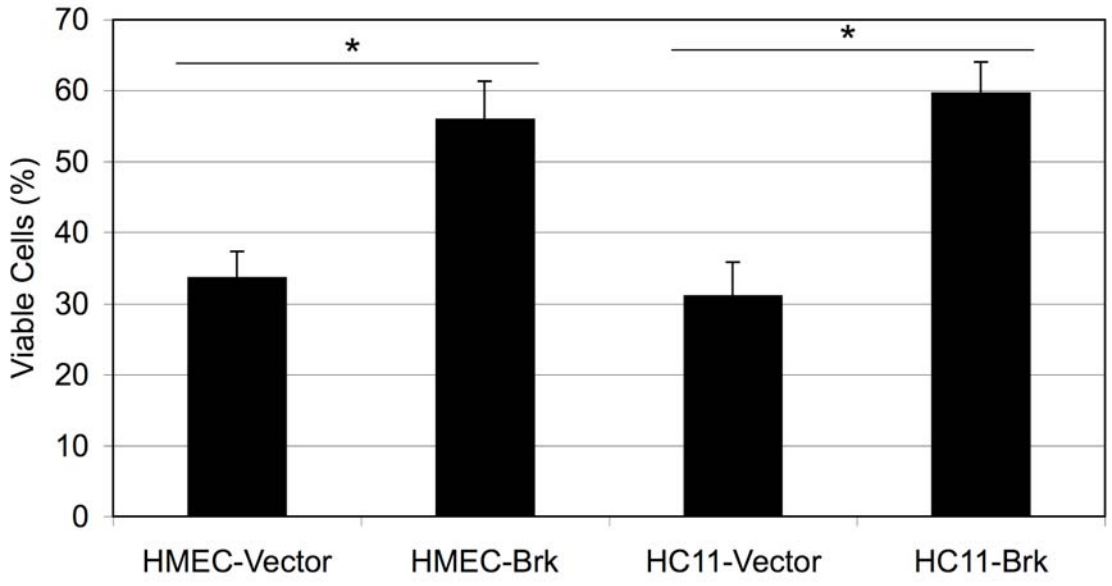

Figure 3.6. Brk promotes anchorage independent survival. HMEC cells stably expressing either a vector (HMEC-Vector) or wild-type Brk (HMEC-Brk), and HC11 cells transiently transfected with vector (HC11-Vector) or wild-type Brk (HC11-Brk) were plated on PolyHEMA coated tissue culture dishes for 48h. Non-adherent cells were collected, trypsinized to disrupt any cell clumps and stained with Trypan blue. Viable cells were determined by dye exclusion. Each condition was plated and counted in triplicate. *p<0.05

the tissue culture plastic. After 48 hours in suspension culture, cells were collected, briefly trypsinized to disrupt any cell clumps, and assayed for viability by Trypan Blue dye exclusion (fig. 4.5). In HMECs, anchorage independent survival increased from 33.8% in cells expressing the vector, to 56.1% in cells expressing Brk. This phenotypic change also appeared in HC11 cells, where survival increased from 31.2% to 59.8% upon Brk expression. These data illustrate the ability of Brk to promote cellular survival in a context that induces apoptosis in non-transformed epithelial cells.

WAP-Brk mice develop adenosquamous carcinoma

Numerous *in vitro* studies suggest that Brk acts as a breast oncogene based on its ability to augment breast cell proliferation, migration and anchorage independent growth. However, this body of work has relied heavily on RNAi approaches primarily performed in transformed and tumorigenic Brk-positive breast cancer cell lines. Experiments expressing Brk in non-transformed mammary epithelial cells have been successful in promoting some aspects of the malignant phenotype, but cooperating factors were usually involved. For example, Kamalati et al. (35) demonstrated Brk-induced soft-agar colony formation in the EGFR-high non-transformed cell line HB4a. Co-expressing Brk and ErbB2 in MCF-10A and pluripotent Comma-1D murine mammary epithelial cells, Xiang et al. (37) showed acinar disruption in matrigel assays of MCF-10A cells and increased tumor growth with orthotopic injections of Comma-1D cells. We aged retired, multiparous WAP-Brk and wild-type breeder mice to determine if Brk expression acts as a potential singular oncogenic insult in the mammary gland. Notably, mammary tumors were infrequent events, but developed in multiparous WAP-Brk mice at a three-fold higher incidence relative to wild-type mice (fig. 3.7a). The average age of tumor onset decreased by roughly 50 percent. The pathology of the tumors consisted of duct-like structures with squamous metaplasia filling the lumens, surrounded by fibrotic stroma (fig 3.7b, left). Keratin pearls were often present (fig. 3.7b, arrows) in lesions where the squamous metaplasia predominated. Large pleomorphic nuclei were evident in these regions. Hyperplastic ducts were also detected in nearby regions of otherwise normal

tissue architecture (fig 3.7b, right). Brk transgene expression was detected in the mammary tumors with strong cytoplasmic staining and sporadic nuclear staining in hyperplastic ducts; weak cytoplasmic staining occurred in cells that had undergone squamous metaplasia (fig 3.7b, right).

Additional immunostaining was performed to determine if the STAT5 and p38 signature seen in HC11 cells is associated with tumor growth in WAP-Brk mice (fig. 3.7c). Phospho-STAT5 and phospho-p38 MAPK IHC revealed strong nuclear staining in Brk-positive hyperplastic regions, and to a lesser extent in the squamous compartments of the WAP-Brk tumor relative to a wild-type tumor (fig. 3.7c, upper panels). The presence of active STAT5 and p38 MAPK establishes a tumor signaling profile that suggests a proliferative lesion, with the exception of the terminally differentiated squamous compartment.

Fig. 3.7: WAP-Brk mice develop mammary tumors

a.

Line	Incidence	Mean Age of Tumor Mice	Mean Parity (Tumor Mice)
Wild Type	0.095 (2/21)	608 days (552d, 665d)	3 litters (3)
Brk^{Low}	0.300 (6/20)	316 days (150d-453d)	1.5 litters (0-4)

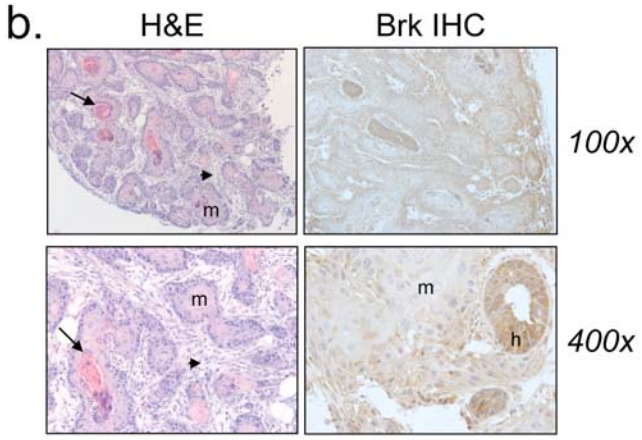

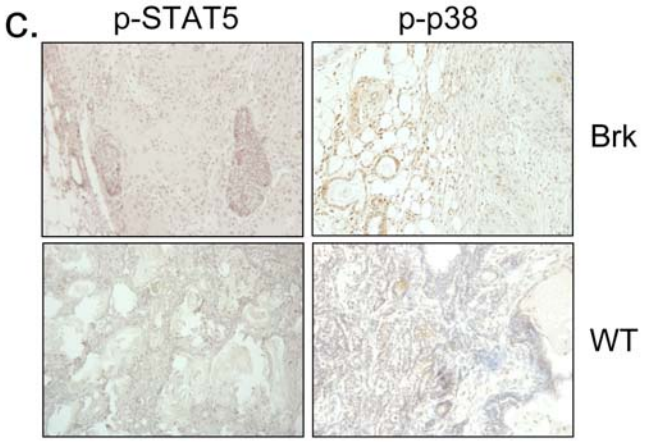

Figure 3.7. WAP-Brk mice develop mammary tumors. *A*, Incidence chart outlining overall incidence, average age of mice developing a tumor, and the parity of the tumor cohort. *B*, Representative images of WAP-Brk tumors. *Left*: H&E sections of an R2 mammary tumor from mouse number B257. *Right*: Transgene expression in the same tumor. (*Arrow: keratin pearl; arrowhead: fibrotic stroma; h: hyperplastic duct; m: squamous metaplasia.) C*, IHC characterization of signaling in a tumor from mouse number B257 (Brk) compared to a tumor from an FVB mouse (WT).

Brk Signaling Intermediates are Evident in Human Breast Biopsies

Although studies are limited, Brk appears to be expressed in a majority of human breast cancers (1), and is often co-expressed (108) or co-amplified (37) with Her2. Using a human breast tumor tissue array, we examined Brk co-expression with phospho-STAT5 and phospho-p38 MAPK in IHC-stained sections of normal breast tissue from reduction mammoplasty (normal breast), fibroadenoma, and infiltrating ductal or lobular carcinoma. Positively-stained sections were also further scored for intensity (by pathological criteria defined in Materials and Methods) (fig. 3.8). As predicted, Brk protein expression (fig. 3.8a) was not detected in normal tissue samples (0/43), and occurred in only one of 41 fibroadenoma samples. However, we detected Brk in 72.5% (29/42) of ductal carcinoma samples and 52.2% (24/46) of lobular carcinomas included in the array. These figures are in agreement with our previous report of Brk expression in up to 86% of mammary carcinoma (of 250 samples; (1)). Notably, phospho-STAT5 (fig. 3.8b) was present in just under half of the normal breast samples (16/34, 47.1%), but low in fibroadenoma (2/30, 6.7%). In contrast to fibroadenoma, ductal carcinoma (25/39, 64.1%) and lobular carcinoma (15/31, 48.4%) expressed moderate to high levels of phospho-STAT5. Similar to Brk expression, phospho-p38 MAPK (fig. 3.8c) was absent from normal breast tissue. However, at least 30% (12/40) of fibroadenoma, 17.9% of ductal samples (7/39), and 37% of lobular carcinoma samples (17/46) stained positively for phospho-p38 MAPK. Representative images of staining intensities appear next to each bar graph for each antibody used in the IHC analysis (fig. 3.8a-c).

We next examined the frequency of co-staining for Brk, pSTAT5 or phospho-p38 within the same samples (fig. 3.8d). Several ductal carcinoma samples that stained positive for Brk also co-stained with either pSTAT5 (59.5%) or phospho-p38 MAPK (18.4%). Approximately 14% of samples stained positive for all three proteins. Of the lobular carcinoma samples, 17.4% of Brk positive samples were also positive for pSTAT5, while 15% of samples co-expressed Brk and phospho-p38 MAPK (7/46). Interestingly, all lobular carcinoma samples exhibiting phospho-p38 also displayed STAT5 phosphorylation. These data suggest that Brk is significantly associated with activated STAT5 and p38 in human breast cancer relative to the normal breast (by χ^2 analysis). Brk signaling to p38 MAPK and STAT5 may characterize a subset (~14-15%) of human ductal and lobular breast carcinoma. More studies are needed to fully understand the contribution of these pathways to the development and maintenance or progression of human breast carcinoma.

Fig. 3.8: Signaling Profile of Breast Tumors

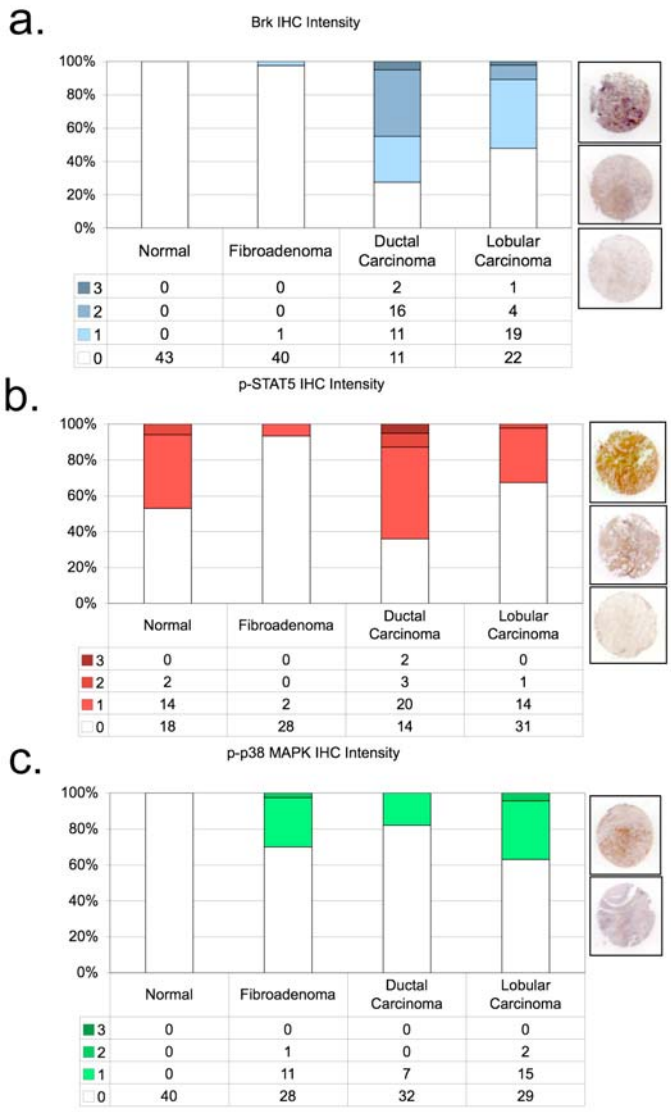

d.

	Brk+p-STAT5	Brk+p-p38	Brk+p-STAT5+p-p38
Normal	0/37	0/35	0/33
Fibroadenoma	0/30	0/39	0/30
Ductal Carcin.	22/37	7/38	5/36
Lobular Carcin.	8/46	7/46	7/46

Figure 3.8. Brk-mediated signaling events are present in a human tissue array. *A*, Brk expression in a human tissue array. *Graphs*: Brk IHC intensity was scored (0-3) and plotted as a fraction of all tissue samples on the array, totaling 100%. L-R: Normal, Fibradenoma, Ductal Carcinoma, Lobular Carcinoma. *B*, Phospho-STAT5 IHC in human tissue array. *C*, Phospho-p38 MAPK IHC in human tissue array. *Images*: Representative images of 1, 2, and 3 intensities for Brk and p-STAT5, 1 and 2 intensities for p-p38. Images shown are from ductal carcinoma samples. *D*, Co-expression pattern.

DISCUSSION

Herein, we report the first transgenic mouse model of mammary specific, WAP inducible Brk expression (fig. 3.1). We demonstrate a delay in mammary gland involution following forced weaning, as evidenced by a lag in characteristic mammary gland morphological changes (i.e. decreased apoptotic figures shed into luminal spaces and a lagging decline in milk production) coincident with increased mammary epithelial cell content, decreased caspase 3 cleavage, and diminished STAT3 phosphorylation during early involution time points (figs 3.1, 3.2, 3.3). We detected evidence of Brk-mediated signaling through increased phospho-STAT5 and phospho-p38 MAPK, in WAP-Brk transgenic mammary tissue (fig. 3.4) and in Brk-transfected HC11 cells (fig. 3.5). Increased activity of these effectors may be responsible for increasing cellular survival in response to the mammary lactogen, prolactin, in the context of the non-transformed mammary epithelium. Brk expression also partially prevented anoikis in non-transformed HMEC and HC11 cell lines *in vitro* (fig 3.6). Aged, multiparous WAP-Brk mice exhibited a higher tumor incidence than wild-type mice; these tumors were Brk-positive and contained high levels of phospho-STAT5 (day 6) and -p38 MAPK (days 4-6) relative to uninvolved adjacent tissue (fig. 3.7). Finally, we detected a signature of high STAT5 and p38 activity in biopsies of Brk-positive human breast cancer (fig. 3.8). Through these studies, a novel mouse model of Brk expression has been created and characterized. Our studies suggest that Brk confers one or more pro-survival signals to non-transformed (luminal) mammary epithelium. Given time, these events may conspire to induce or permit the formation of latent mammary tumors (fig 3.7).

Involution: *In vivo* modeling of mammary oncogenesis often begins with overexpression of potential breast oncogenes or targeted deletion of tumor suppressor genes. By examining the tightly regulated process of mouse mammary gland involution in the presence of a transgene, subtle alterations in pro-survival or proliferative cellular pathways are often revealed. Indeed, this complex biological process in the mouse represents a highly sensitive readout of human oncogenic action; numerous breast oncogenes (including Akt (93), Bcl2 (94), and EGFR (95) induce delayed involution in mouse models (reviewed in (109)). In this study, we have illustrated a modest, but functionally significant, survival advantage conferred upon Brk expression in mammary epithelium that results in delayed post-weaning mammary involution. Similar to other models of mammary oncogene expression (93-95), our model undergoes delayed, but ultimately complete mammary regression, highlighting a distinct window of mammary signaling events (in our case, days 4 to 6 of involution) that are perturbed without completely halting the involution process. We observed fewer apoptotic figures and decreased caspase3 cleavage in WAP-Brk transgenic glands. Notably, clearance of apoptotic mammary epithelial cells does not appear to be affected since WAP-Brk transgenic mice eventually undergo complete mammary regression, implying that Brk-mediated survival is initially a transient phenomenon, largely revealed in the context of early involution. With multiple rounds of parity induced mammary expansion and contraction, the effects of a transient survival event likely become amplified, increasing the chances for cells to encounter and fix potentially oncogenic combinatorial events.

Brk mediated signals: Separating normal physiological cues from transgene-mediated signaling is critical to understanding events that may contribute to mammary oncogenesis. Initial characterization of WAP-Brk mammary glands focused on STAT3 signaling as a marker of mammary gland involution. STAT3 is a required mediator of involution-related cell death (89), and has been reported to be a Brk substrate in studies using cell lines (22). We observed apparent suppression of STAT3 phosphorylation (as indicated by the lack of total "shifted" STAT3 in SDS-PAGE gels) in Western blots of purified mammary epithelial cells from WAP-Brk-transgenic glands (fig 3.1), and IHC illustrated that WAP-Brk glands contain less p-STAT3 during involution (days 4, 6) relative to wild-type glands (fig. 3.3b). These results suggest that Brk mediated STAT3 phosphorylation may serve a prominent role in established mammary tumors (i.e. breast cancer cells; (110)), but is not necessarily physiologically relevant during the initiation of involution, when altered by Brk expression. That is, Brk does not appear to be a positive regulator of STAT3 *in vivo*; STAT3 phosphorylation serves primarily as an indicator of the progress of mammary involution herein.

Weaver et al., (23) reported that Brk-positive breast cancer cell lines have elevated p-STAT5, and that STAT5 is a Brk substrate *in vitro*. Our studies show that Brk expression *in vivo* also promotes STAT5 phosphorylation (fig. 3.4a), most likely by sensitizing cells to the lactogenic ligand, prolactin (fig. 3.5). Walker et al. (110) have illustrated that transiently or constitutively activating STAT5 is a dominant signal (relative to STAT3) in breast cancer cells. Clarkson, et al.. al. (111)specifically, have

shown that p-STAT5 is sufficient to attenuate apoptosis even in the presence of p-STAT3. In this context (i.e. the intact mammary gland), Brk may amplify physiologically dominant STAT5-mediated survival *in vivo* (i.e. relative to STAT3 *in vitro*).

We have previously described Brk mediated p38 MAPK signaling as primarily promoting cell migration in EGF or heregulin-treated breast cancer cell lines (1). There are limited studies investigating the role of p38 MAPK activity in mouse models of breast cancer. Demidov, et al. (112) expressed an MMTV-driven active MKK6 (an upstream kinase in the p38 MAPK module), and showed resistance to development of ErbB2 and Wip1 induced mammary tumors; however when overexpressed, MKK6 can likely regulate other MAPKs (113). Similar to our studies, Leung et al. (97) expressed MMTV-V12Rac3 and described incomplete involution associated with elevated phospho-p38 MAPK. Additionally, Wang et al. (114) overexpressed activated Pak1 under the β-lactoglobulin promoter and reported a 20% tumorigenesis rate and elevated phospho-p38 MAPK. In both of these studies, as well as ours, there were detectable levels of phospho-p38 in wild-type cohorts, strongly suggesting an as of yet undescribed physiological role for p38 MAPK in mammary involution. Our WAP-Brk transgenic mammary glands exhibited higher phospho-p38 levels relative to wild-type glands during days 4 and 6 of the involution time course (fig. 3.4b), again consistent with increased survival stimulus in WAP-Brk mice. Interestingly, expression of Brk in HC11 cells increased basal phospho-p38 in serum-starved cells (fig. 3.5), indicating that the presence of Brk is sufficient to promote p38 MAPK activation and survival of mammary epithelium. Thus p38

phosphorylation induced by Brk expression in non-transformed mammary epithelium could contribute to breast disease as either an early event (allowing migration/dissemination or luminal filling) or late event (therapy resistance) in tumorigenesis, thereby leading to a poor prognosis. Recent literature (40, 107) and our observations in HMEC and HC11 cell lines (fig. 3.5) illustrate that Brk promotes anchorage independent survival. Importantly, this has been shown to be a p38 MAPK dependent phenotype in Brk positive MDA-MB-468 cells (115). Taken together, these data suggest that Brk-mediated p38 activation is likely a critical node for cell pro-survival and relevant to early oncogenic signaling; p38 inhibitors may present an opportunity for therapeutic intervention aimed at long term breast cancer prevention.

Tumor Biology (in vivo model and human tumors): Brk expression in our WAP-driven transgenic model results in a tumorigenesis rate of 30% in aged multiparous mice (fig 3.7). Two wild-type FVB mice from the same liter also developed tumors. Indeed, this strain has a weak propensity to develop adenosquamous mammary tumors at an advanced age (116). Because of the two wild-type FVB tumors, the comparison of the number of tumors between WT and Brk transgenic animals did not reach statistical significance ($p=0.13$). However the age at tumor onset was nearly halved (fig. 3.7a), indicating an effect of Brk expression on the promotion of tumorigenesis relative to wt FVB mice. Brk strongly promotes breast cancer cell proliferation, survival and migration *in vitro* (1, 21, 31, 39). We did not observe metastatic lesions in tumor-bearing WAP-Brk mice, suggesting that other cooperating factors are necessary for invasion and migration *in vivo*.

We are currently investigating WAP-Brk experimental interaction with other mouse models of breast cancer in order to identify additional oncogenic events that may cooperate with Brk overexpression.

Brk protein is readily detectable in hyperplastic regions of WAP-Brk mammary tumors (fig. 3.7b). The loss of Brk protein in regions of squamous metaplasia of WAP-Brk tumors is likely due to the loss of mammary epithelial differentiation, an event(s) that may ultimately lead to silencing the WAP promoter. Note that Brk expression may drive the appearance of the squamous metaplasia phenotype directly, as Brk expression in the skin increases during the maturation of keratinocytes, promoting squamous differentiation of the epidermis (117).

Brk appears to predominantly mediate cellular survival/resistance to involution-associated apoptosis in this model. This phenotype is consistent with Brk-dependent activation of STAT5 and p38 MAPK (1, 23), as measured by their increased phosphorylation (figs 3.4-7). Elevated p-STAT5 (day 6) and phospho-p38 (days 4 and 6) are detected in our involution time course experiments, *in vitro* experiments with Brk-expressing HC11 cells, and in Brk+ tumors derived from both WAP-Brk mice and humans. As expected, IHC analysis of the human breast tumor tissue array revealed Brk expression in only one (a fibroadenoma) of the 84 non-transformed tissue samples (fig. 7a), and in Brk+ tumors, was associated with increased p-STAT5 (fig. 7b) and to a lesser degree phospho-p38 (fig. 7c). However, expression of phospho-p38 was only associated with abnormal breast pathologies. Interestingly, phospho-STAT5 was detected in nearly 50 percent of the normal breast tissue, likely due to normal circulating prolactin levels

during the menstrual cycle; the samples in this group were mostly derived from premenopausal women (118).

As a whole, these results highlight a previously undescribed cellular signaling axis that decreases the efficacy mammary gland involution (a well controlled cell death process) and promotes tumorigenesis in a model. Further investigation of the Brk/STAT5/p38 signaling axis in non-transformed mammary tissue could likely define a novel route to malignant transformation, and may serve as a route for therapeutic intervention in the future.

Acknowledgements

We would like to thank Dr. Ilze Matise (Comparative Pathology Core, Masonic Cancer Center, University of Minnesota) for initial pathology consults, Dr. Jeff Rosen (Baylor College of Medicine) for the gift of the WkbpAII transgene vector, Abby Olsen for preparing the transgene, and Jonathan Henriksen (BioNET Digital Imaging Facility, University of Minnesota) for digital imaging analysis.

Co-authors on this study included Dr. Daniel Housa (IHC, tumor array construction, pathology analysis), Gregory K. Hubbard (IHC, mouse colony management, and mammary epithelium preparations), and Dr. Kathryn L. Schwertfeger (discussions and assistance with experimental planning).

Funding was provided by NIH/NCI R01 CA107547 (to CAL) and Department of Defense Pre-doctoral Fellowship BC061473 (to KAL).

CHAPTER 4

IN VITRO MODELING OF BRK-MEDIATED EVENTS

INTRODUCTION

Brk belongs to a family of soluble kinases similar to cSrc. As such, Brk phosphorylation and kinase activity can be induced by growth factor receptor signaling cascades. Upon ligand binding to its cognate receptor, growth factor receptors (GFRs) dimerize and transphosphorylate, activating their kinase activity and recruiting adapter molecules and scaffold proteins to potentiate receptor-mediated signaling.

Although GFR pathways exhibit a degree of redundancy, a multitude of ligand-induced signaling events exist that occur in a context dependent manner. For example, treating the prostate hyperplasia cell line BPH-1 with epidermal growth factor (EGF) results in a Brk-dependent activation of Akt (34), but EGF treatment of SKBR3 or T47D breast cancer cells induces Akt phosphorylation independent of Brk expression (1). Differential effects of Brk activity in cell biology can be explained by ligand specificity as well. For example, hepatocyte growth factor (HGF) treatment of HaCaT cells results in Brk mediated migration, however treatment with macrophage stimulating protein (MSP) does not induce cellular migration though it does induce Brk kinase activity (39).

When expressed in non-transformed tissues, Brk primarily has a growth suppressive role, either by inhibiting the activity of proliferative signaling molecules or the induction of apoptosis in response to DNA damage (41) (42).

Ligand/receptor interactions able to induce Brk kinase activity include epidermal growth factor (EGF) activation of EGFR (21), heregulin-β1 (HRG) induced ErbB receptor activation (1), IGF1 receptor signaling (107), and most recently hepatocyte

growth factor (HGF) and macrophage stimulating protein (MSP) activation of the cMET and RON receptors, respectively (39).

Context and ligand dependent biology is highlighted in mammary gland developmental and morphogenic processes. Temporospatial signaling via growth factors and hormones induces differential biology (duct elongation vs. branching, alveolar expansion vs. functional differentiation). Models have been developed to investigate context dependent cues in mammary morphogenesis in vitro, one of which utilizes the extracellular matrix components laminin, collagen IV, and heparan sulfate proteoglycans (119) to mimic the environment necessary for organogenesis/mammary differentiation. Cells receive survival cues from the microenvironment by establishing apicobasal polarity through integrin-mediated ECM attachment. These cues are critical for regulating luminal hollowing, which relies on the induction of cell death induced by loss of ECM anchorage of the interior cells in mammary spherioids. Alteration of signaling events during this process often result in cell biology that mimics initial steps seen in oncogenesis of the breast: anchorage independent growth resulting in filling of the mammary lumen, loss of cellular polarity, and/or disruption of cell-cell junctions.

In this chapter, we examine the effects of Brk expression on growth factor (EGF, HRG, HGF) and peptide hormone (PRL) induced signaling events. Additionally, *in vitro* phenotypic changes in cell biology are investigated in physiologically relevant contexts that mimic those seen in mammary gland development and malignancy.

RESULTS

Brk expression in HMEC cells does not influence mammary organoid hollowing

Because Brk promotes cell survival in an anchorage independent culture method (fig. 3.6 and(40, 107)), we hypothesized that Brk expression would decrease cell death in the lumens of organoids when mammary epithelial cells were cultured on laminin-rich basement membrane (lrBM, commercially available as Matrigel). Human mammary

Fig. 4.1: HMEC-Brk Organoids Undergo Luminal Hollowing

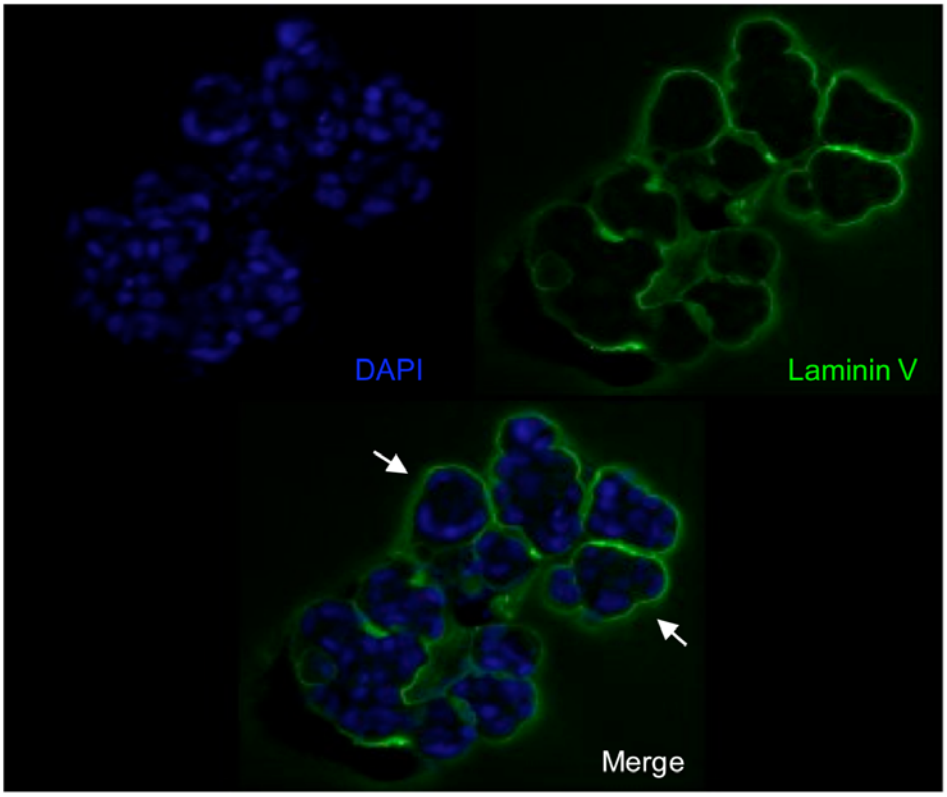

Figure 4.1. HMEC stably expressing wild-type Brk were plated on solidified Matrigel, and overlaid with complete growth medium containing 2% Matrigel. The overlay medium+Matrigel was changed every two days for a total of 12 days. Immunofluorescence was performed using anti-Laminin V antibody and DAPI. Image is a colorized composite of a frame capture from a confocal Z stack at 400X magnification.

epithelial cells (HMEC) engineered to express Brk (83) were seeded on solidified Matrigel, and overlaid with MEGM containing 2% Matrigel. The overlay medium was replaced every two days for twelve days, when cultures were immunostained and imaged with a confocal microscope (fig. 4.1). DAPI stained DNA indicates nuclei (fig. 4.1, blue), and laminin V immunofluorescence outlines the basal surface of individual organoids (fig. 4.1, green). HMEC-vector and HMEC-Brk cultures were comparable when compared by eye, forming colonies of roughly similar size in the Matrigel. When the cross-section of an organoid is in the focal plane (indicated by the arrows), it is evident that HMEC-Brk cells undergo complete luminal hollowing (as do HMEC-vector cells, not shown) illustrated by the absence of nuclei on the interior of the spherical structure. These data show that Brk expression is not sufficient to disrupt alveolar/organoid morphogenesis *in vitro*.

Brk expression decreases doxorubicin induced cell death

In addition to sensitizing cells to growth factor stimulation (36), a recent study by Xiang et al(37)has shown that Brk expression confers increased survival by decreasing the efficacy of Lapatinib treatments in MCF10A cells overexpressing ErbB2. Other studies have implicated Brk in cellular survival through the phosphorylation of signaling proteins downstream of Brk activation (Erk5 and p38 in (1), ErbB3 in (36)). However, literature also exists in which Brk sensitizes non-transformed intestinal epithelium to apoptosis (120) and suppresses EGF induced proliferation in HMECs (83). Using our HMEC cells stably expressing Brk, we performed a cell death assay to determine whether

Fig. 4.2: Brk Expression Partially Inhibits Doxorubicin Induced Cell Death

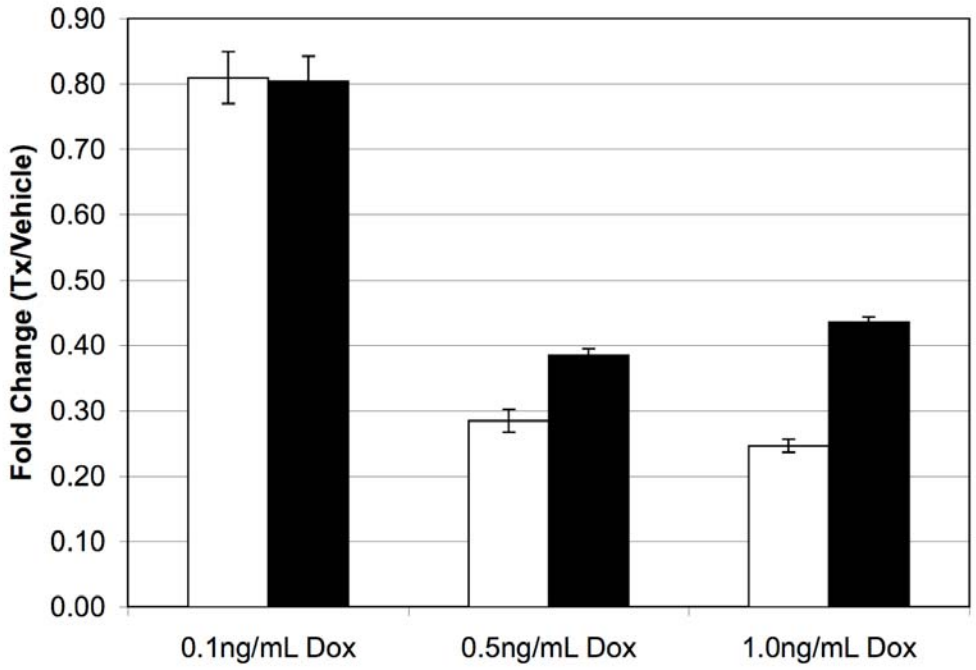

Figure 4.2. HMEC cells engineered to stably express vector or wild-type Brk were plated in 24 well plates and treated for 18h with 0.1ng/mL, 0.5ng/mL, and 1.0ng/mL doxorubicin. After a 16h incubation with the drug, viable cells were quantified with a colorimetric MTT dye conversion assay, and normalized to the vehicle control cells at the 16h timepoint.

Brk expression is sufficient to promote cellular survival in non-transformed mammary epithelium.

At a dosage of 0.1ng/mL doxorubicin, no significant difference between HMEC-vector cells and HMEC-Brk cells was detected, with approximately 80% of plated cells remaining viable relative to vehicle treated controls (fig. 4.2). At doxorubicin dosages of 0.5ng/mL and 1.0ng/mL, however, HMEC-Brk cells remained approximately 40% viable, whereas HMEC-vector cells were 25-30% viable relative to vehicle controls. These results suggest that Brk expression in HMEC cells provides a slight survival advantage in the presence of cytotoxic therapy that induces DNA damage.

HGF and EGF Induce Changes in Brk localization in a Breast Cancer Cell Line

Previous studies have documented the localization of Brk in various tumor types and cell lines. Normal prostate epithelium and well-differentiated prostate tumors express Brk in the nucleus, whereas poorly differentiated and aggressive prostate cancer cells exhibit cytoplasmic staining (17). However, in B and T cell lymphomas, Brk expression is nuclear (15). Additionally, in HEK-293T cells, Kim and Lee (121) have illustrated that the oncogenic functions of Brk (proliferation, survival and focus formation) are abolished when Brk is targeted to the nucleus, and enhanced when targeted to the plasma membrane. These studies suggest that Brk localization and activity is cell-type specific, and "transformation-state" dependent (malignant vs. normal).

In order to compare localization of endogenous, growth factor activated Brk in non-transformed HaCaT keratinocytes and MDA-MB-231 breast cancer cells were serum starved, treated for 30 or 60 minutes with various growth factors, and subjected to immunofluorescence using an anti-Brk antibody (fig. 4.3). Brk expression in untreated HaCaT cells presented as diffuse cytoplasmic and nuclear staining, whereas untreated MDA-MB-231 cells were predominantly cytoplasmic, with some accumulation in the perinuclear space. Upon 30 minutes of treatment with HGF, EGF or IGF (which does not activate Brk in an *in vitro* kinase assay (1) localization did not change in HaCaT cells. However, in MDA-MB-231 cells, HGF dramatically increased perinuclear accumulation. EGF induced diffuse Brk appearance in the nucleus, while IGF induced a slight decrease

in perinuclear localization compared to the basal state. At 60 minutes of HGF or IGF treatment, Brk localization did not change in HaCaT cells (EGF was not tested), however a slight increase in nuclear intensity was noted with HGF, although this was not quantified. In MDA-MB-231 cells, perinuclear staining intensity continued to increase with HGF, and began to accumulate in response to IGF treatment. These results suggest not only cell type specific localization patterns, but specificity of growth factor induced Brk localization and kinetics. Additionally, these data illustrate the strong potential for differences between Brk-mediated signaling in normal vs. malignant cell lines and tissues.

Fig. 4.3: Brk Localization in Response to Growth Factors

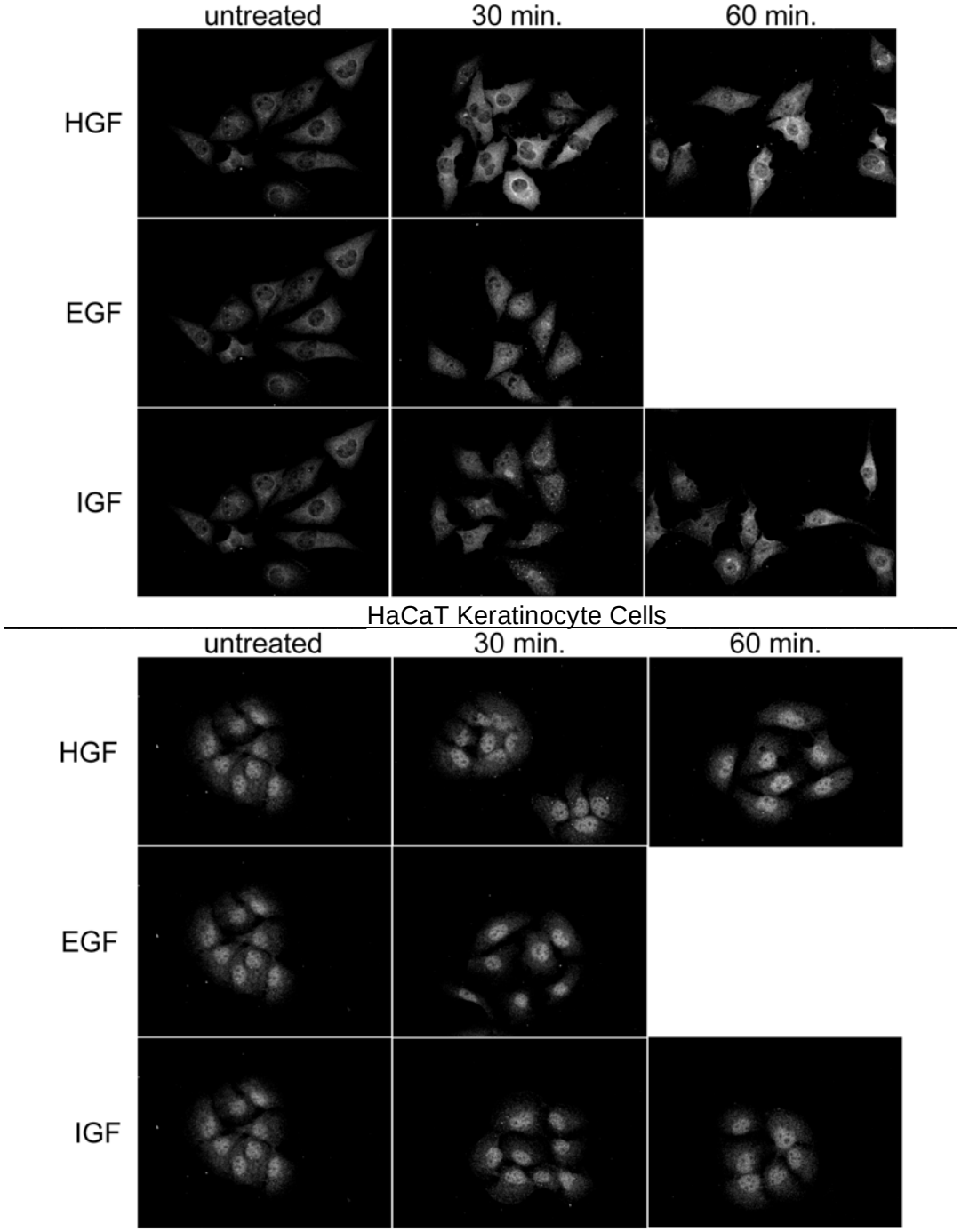

Figure 4.3: Brk localization changes in response to growth factor stimulation. MDA-MB-231 breast cancer cells or HaCaT keratinocyte cells were cultured on glass coverslips, serum starved, then treated with HGF, EGF, or IGF for 30 or 60 minutes and fixed. Immunostaining was done with anti-Brk primary and AlexaFluor488 conjugated secondary.

Brk Mediates Heregulin Induced Erk5 and p38 MAPK Activation in Cancer Cells

It is known that Brk activity is induced by EGF treatment and ErbB receptor activation, such as ErbB2, the target of trastuzumab (trade name Herceptin). Delineating Brk-mediated signaling events downstream of ErbB receptors will allow the identification of signaling molecules that may confer therapy resistance. In studies initiated by Dr. Julie Hanson Ostrander to identify signaling events mediated by Brk in breast cancer cells, we stably transduced multiple cell lines with shRNA directed to Brk, in order to knock-down Brk expression. After selection of Brk knockdown pools, we treated cells with EGF or HRG for 5 to 60 minutes. Western blotting for phospho-Akt, phospho-Erk1/2, and phospho-JNK did not show any differences between T47D cells expressing negative control shRNA or Brk shRNA, however phospho-Erk5 and phospho-p38 MAPK were decreased in the Brk knockdown cells relative to controls (fig. 4.4a). To validate this result, HRG was used to treat SKBR3 cells stably expressing control shRNA or Brk shRNA, and lysates were blotted for phospho-Erk5 and phospho-p38MAPK. As in the T47D cells, Erk5 and p38 MAPK phosphorylation was decreased in Brk knockdown cells (fig. 4.4b). Treating T47D cells with interleukin-1β, which activates the p38 MAPK mediated inflammatory response, did not rely on Brk expression, indicating a HRG induced, ErbB receptor specific difference in the mechanism of p38 MAPK phosphorylation (fig. 4.4c).

Fig 4.4: Brk mediates Erk5 and p38 MAPK phosphorylation

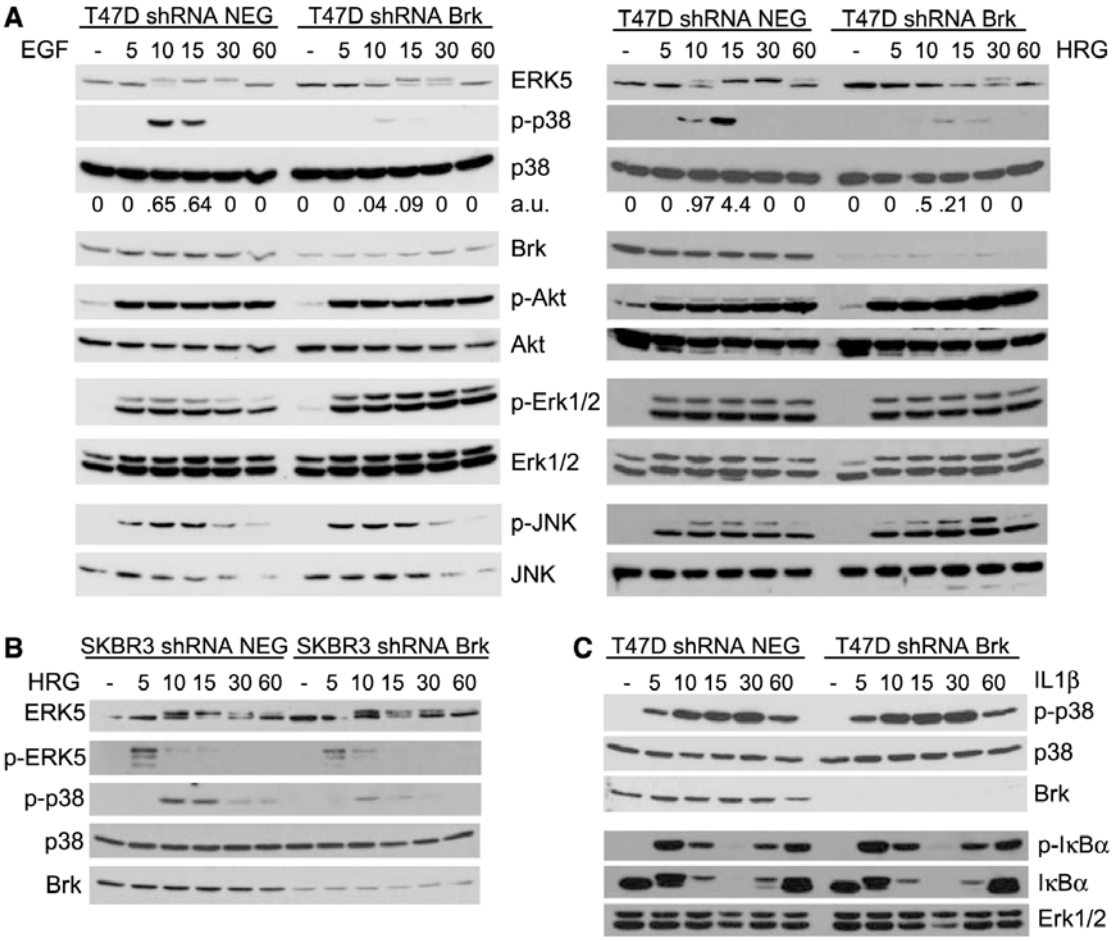

Figure 4.4. Brk promotes Erk5 and p38 MAPK phosphorylation in breast cancer cell lines. *A*, T47D breast cancer cells stably transduced with Brk-specific or negative control shRNA were serum starved then treated with 25ng/mL EGF or heregulin (HRG) for 5, 10, 15, 30 or 60 minutes. Whole cell lysates were blotted for Erk5, Brk, and phospho- and total-p38 Akt, Erk1/2, and JNK. Densitometry results of phospho-p38 MAPK inhibition (relative to total p38 controls) are shown under the total p38 MAPK blot in arbitrary units (a.u.). *B*, SKBR3 breast cancer cells stably transduced with Brk-specific or negative control shRNA were serum starved then treated with 25ng/mL EGF or heregulin (HRG) for up to 60 minutes. Cellular lystates were blotted with antibodies for phosphorylated and total Erk5, phospho- and total p38 MAPK, and Brk. *C*, T47D cells expressing Brk or negative control shRNA were treated with 5ng/mL IL-1β for up to 60 minutes. Cell lysates were Western blotted for phospho and total p38 MAPK, Brk, phosphorylated and total IκBα, and Erk1/2. (adapted from (1) #1355}

DISCUSSION

In this chapter, Brk expression does not impair luminal hollowing in a 3D culture system with ECM components present (fig. 4.1). Interestingly, Brk expression in HMEC cells did confer decreased sensitivity to doxorubicin treatment (fig 4.2). Through confocal imaging, Brk localization in response to treatment with HGF, EGF and IGF illustrated that each ligand results in differential Brk translocation kinetics in a timecourse of ligand treatment (fig. 4.3). Altered kinetics were seen when comparing the Brk-positive MDA-MB-231 breast cancer cell line to HaCaT keratinocytes, a non-transformed cell line that exhibits endogenous Brk expression (fig. 4.3). Heregulin and EGF treatment in the presence of Brk knockdown in T47D and SKBR3 breast cancer cells revealed a requirement for Brk in Erk5 and p38 MAPK activation, as measured by their phosphorylation (fig. 4.4).

These experiments illustrate the variety of ligands capable of activating Brk-mediated signaling events and/or the resulting biology, which, through continued investigation, will contribute to further understanding mechanisms behind cellular events that promote malignancy. Because Brk is a kinase, *in vitro* models for Brk-mediated signaling events have focused primarily on activation of Brk kinase activity, either through ligand induced signaling (1, 36) or mutations that affect Brk kinase activity (12, 39). This chapter along with the studies of others highlight that, in addition to ligand specificity and duration of signal activation, context mediated biology is a required consideration when interpreting Brk mediated events *in vitro* (17, 121, 122).

Specificity of ligand mediated Brk signaling: Each ligand used to stimulate Brk mediated signaling in this chapter has a distinct function ascribed to it, all of which are involved in normal mammary gland biology. These pathways are often inappropriately regulated during (or as a result of) the malignant transformation process. For instance, in a normally developing mammary gland, EGF and IGF are required to induce ductal outgrowth, and HRG and HGF promote ductal branching (123, 124). The fact that there are several redundancies in growth factor mediated biology in mammary development speaks to the importance of sufficiently coordinating proliferative and migratory signals.

EGF- and HRG-mediated Brk signaling activate a common signaling node in breast cancer cells (fig 4.4), resulting in Erk5 and p38 phosphorylation and activation. With HGF treatment, Erk5 activation is seen, but p38 is not well activated (39). Additionally, prolactin treatment is able to phosphorylate p38 MAPK in a Brk dependent manner (fig. 3.5). These data suggest that in non-transformed mammary epithelium, p38 MAPK is a significant node in Brk mediated signaling events that may promote tumorigenesis by an HGF independent mechanism (i.e. when Brk is overexpressed), but may support malignancy after transformation by HGF induced signaling. Additional *in vivo* studies are underway to address Brk cooperation with other oncogenes, and also partially address signaling upstream of Brk.

Although Brk is not expressed in normal mammary epithelial cells, it is likely that aberrant Brk expression co-opts normal growth factor signaling to promote surivival (via p38 MAPK) and/or proliferation (STAT5). The phosphorylation of these signaling molecules is clearly promoted by Brk in breast cancer cells (1, 23), and when Brk is

overexpressed in HC11 cells (fig. 3.5). Because PRL, HRG, and EGF are present (and required) in the normal mammary gland, a small number of Brk positive cells capable of activating p38 MAPK and STAT5 would gain a survival advantage over normal, Brk null cells early in tumorigenesis.

Sub-cellular localization of Brk changes in a ligand specific manner: With the exception of prolactin, the ligands used in this chapter have all been shown to induce Brk kinase activity (EGF (21), HRG (1), HGF (39), potentially acting through selective use and specificity of scaffolding and adaptor molecules. Just as sequestration of growth factor production to fibroblasts regulates paracrine effects on the nearby epithelium (125), the intracellular localization of signaling molecules can regulate signaling function or activity (126). Previous studies have illustrated that Brk can exist in both the cytoplasmic and nuclear compartments of cells (17), however, the localization depends on the tissue (prostate, skin, colon) and degree of malignancy or degree of differentiation (prostate). Because the Brk protein does not have a myristoylation sequence, the detection in both compartments is not surprising, however the biological effects of Brk expression vary based on localization (16, 17, 38). Additionally, Brk lacks a nuclear localization sequence (121), implying interaction with other molecules that undergo nuclear translocation. With the variety of downstream signaling molecules involved in the respective ligand induced pathways, we hypothesized that Brk localization would change with ligand treatment, as the phosphorylated active form of Brk proceeds to interact with growth factor receptors, scaffold proteins, or adaptor proteins.

In the serum starved condition, Brk localization in the MDA-MB-231 cell line was predominantly cytoplasmic, but with a slight perinuclear accumulation (fig. 4.3). After 30 minutes of HGF treatment, slight nuclear staining appeared and perinuclear staining intensified. At 60 minutes of HGF treatment, cytoplasmic staining became punctate and intensely perinuclear, but nuclear entry also became more evident.

Upon 30 minutes of EGF treatment, Brk localization in MDA-MB-231 cells became diffuse in both the cytoplasm and nucleus, illustrating a kinetic difference for nuclear translocation and suggesting a different mechanism for nuclear entry than when cells were treated with HGF. IGF treatment did not dramatically alter Brk localization at 30- or 60-minute treatment durations, suggesting another alternative set of mechanisms for Brk activation. Although Brk was well activated, Brk localization in the non-transformed HaCaT keratinocyte cell line was unchanged at all timepoints with all ligands, relative to the untreated control, suggesting that in non-transformed keratinocytes, Brk compartmentalization is not the primary mechanism for Brk-mediated signaling.

Several studies have implicated that Brk localization has differential effects on cell biology depending on the type of tissue being assayed. Nuclear Brk localization in SW620 colorectal carcinoma cells inhibits β-catenin transcriptional activity, whereas targeting Brk to the membrane increases β-catenin transcriptional activity; this inhibitory role for Brk in β-catenin function was echoed in the $PTK6^{-/-}$ mouse when crossed with a β-catenin reporter transgenic mouse (33). In non-malignant prostate samples, Brk is primarily localized in the nucleus, whereas cytoplasmic and perinuclear staining

increases as prostate tumors become less differentiated (17). This observation is echoed in the limited confocal imaging presented in this chapter. With respect to changes in Brk localization, the non-transformed HaCaT cells did not respond growth factor stimulation (Brk remained nuclear), and in the MDA-MB-231 cells, Brk was initially cytoplasmic, but translocated to the nucleus. Although these model cell lines are not of the same tissue of origin, the use of HaCaT cells are an appropriate model for endogenous Brk expression, as Brk is not detected in our cell stocks of mammary epithelial cell lines HC11, HMEC, or MCF-10A (however, Irie et al (107) has shown Brk expression in their MCF-10A cultures). Additionally, λm5, a truncated splice variant of Brk that lacks kinase activity and has a novel proline-rich region, has been detected in T47D breast cancer cells and PC3 prostate cancer cells (127, 128). Brauer et al. described that although this splice variant is present in PC3 cells, it is not responsible for altering localization of full-length Brk protein by competition for binding proteins that may direct localization changes (128).

Our immunofluorescence assays did not account for signaling intermediates, however future co-localization immunofluorescence would be feasible to investigate the presence of putative molecules present in signaling complexes. Through the creation and use of mutations in the linker and SH3 domains, or by using constitutively active or kinase-dead Brk mutants, binding partners could elucidate binding sites that are required for growth factor induced translocation.

Brk-mediated doxorubicin resistance: Several Brk mediated signaling pathways have been implicated (directly or indirectly) in cellular survival and potential therapy

resistance. Considering that the initiating steps of Brk mediated malignancy are unknown to date, we used HMEC-Brk cells to test whether or not Brk expression would confer a survival phenotype, and therefore, resistance to the cytotoxic drug doxorubicin. This allowed us to determine whether simply expressing Brk in a non-transformed cell line would result in proliferative or survival signal strong enough to overcome apoptotic stimulus (as in (40, 107, 127)), or whether it would sensitize cells to apoptosis (as reported for non-transformed fibroblasts (129) and intestinal epithelial cells (42)). We used an MTT cell viability assay to evaluate Brk-mediated survival, in the presence and absence of doxorubicin, an anthracycline routinely used for cytotoxic chemotherapy.

Figure 4.4 shows a subtle, but higher degree of cellular viability in Brk-positive cells in the presence of doxorubicin, relative to HMEC-vector cells, suggesting that Brk may be a cooperating oncogene rather than a singular oncogenic insult. Because the cells were plated in complete growth medium (MEGM), it is also possible that the effect of Brk expression on HMEC survival may be partially masked due to the abundance of growth factors present in the culture medium. Repeating the assay with growth factor deprivation prior to doxorubicin treatment may accentuate the difference in cellular viability, by introducing additional cellular stresses. An increased doxorubicin dosage was not informative, nor was lengthening the duration of treatment, as both approaches resulted in cellular viability of approximately 10% of the vehicle controls (data not shown). Future experiments may also be able to shed light on whether Brk mediates acquired resistance to anthracyclines rather than primary resistance.

Context dependent anchorage independent survival: The topic of focus in a recent issue of the Journal of Mammary Gland Biology and Neoplasia (volume 15, September 2010), the importance of understanding extracellular cues provided by the mammary stroma is becoming a critical area of study. Numerous studies have shown epithelial cells integrate cues from neighboring cell types and structural components of tissues to determine their appropriate phenotypic response. This is perhaps illustrated best in Kuperwasser, et al (130), where xenografts of human mammary epithelial cells into a cleared murine fat pad did not colonize the gland, whereas injection of human mammary epithelium along with human fibroblasts resulted in engraftment and development of human-like lobular morphogenesis.

In figure 3.5 both HMEC-Brk cells and HC11-Brk cells exhibited an increase in anchorage independent survival when cultured on PolyHEMA, which mimics detachment from the basement membrane and induces anoikis. In this context, Brk expression is promoting a mechanism for cellular survival in the short-term (48 hours). Future experiments will determine if this is through p38 MAPK activation, which we have previously shown is downstream of Brk activation (1) and has recently been implicated in anchorage independent survival (115).

Debnath et al. (85) have described an effective three-dimensional culture technique for developing mammary organoids that closely mimics the process of *in vivo* mammary development, in contrast to cells grown in a monolayer culture. When non-transformed mammary epithelium is cultured on a laminin-rich recombinant basement membrane (lrBM, such as Matrigel), cells form colonies within the lrBM. When cells on

the interior of the colony are no longer in contact with the lrBM, anoikis is induced by the detachment from ECM components. In this assay, 8-day cultures of HMEC-Brk cells did not exhibit increased anchorage independent growth, as lumen formation in 3D mammary organoids was not disrupted (fig. 4.1).

Taken together, the PolyHEMA and the Matrigel assays illustrate the context dependent nature of Brk-mediated phenotypes. When extracellular input is binary (adherent vs. non-adherent) and non-adherent cells are not in contact with each other, Brk is able to promote cellular survival in the short term (fig. 4.5). However, when cells are cultured on Matrigel resulting in cell-cell contact and the added stromal inputs of laminin, collagen IV, and heparan sulfate proteoglycans are present, these signals are integrated in a manner in which apoptosis occurs as usual in cells not attached to the ECM, resulting in lumen formation (fig. 4.6). These data suggest that Brk is sufficient to promote anchorage independent survival, but not anchorage independent proliferation. Also implied is that Brk may exert its oncogenic effects best in cooperation with other initiating events, or that when in the presence of ECM components, the oncogenic effects of Brk are suppressed by integrin and growth factor receptor cross talk as illustrated by Miyamoto et al. (131).

Overall, the data presented in this chapter illustrate that Brk expression in non-transformed mammary epithelium results in promotion of cellular signaling pathways that mediate cellular proliferation and/or cellular survival and potential routes for investigation of these signals. The importance of the context in which Brk-mediated

signaling occurs is illustrated, adding to the theory of distinct proto-oncogenic vs. oncogenic Brk functions in tumor biology. These nuances, however subtle, will need to be fully considered when choosing which model system or tumor profile to use when developing breast cancer therapeutics directed towards Brk or Brk-mediated signaling events.

ACKNOWLEDGEMENTS:

I would like to thank Dr. Julie Ostrander for creating the HMEC-Vector and HMEC-Brk cell lines (83), and leading the studies on heregulin-mediated Brk signaling (1).

CHAPTER 5

CONCLUSION

These studies have described the establishment of a mouse model to investigate *in vivo* Brk/Ptk6 expression in normal mammary epithelium. We demonstrated that mammary specific expression of a WAP-Brk transgene is induced upon pregnancy, and results in delayed post-weaning mammary gland involution and promotes tumorigenesis. Investigation of involution associated cell death revealed that mammary glands from Brk transgenic mice display decreased activation of caspase 3, relative to wild-type controls, during early involution. Additionally, Brk expression in mammary glands results in lower levels of phosphorylated STAT3 in the involuting mammary epithelium, indicating a decreased initiation of involution signaling events. STAT3 and STAT5 phosphorylation in the mammary gland are inversely regulated (25), thus we investigated the effects of Brk expression on STAT5 signaling activation. During involution, the duration of detectable STAT5 phosphorylation was longer than in controls. Phosphorylation of p38 MAPK, a downstream mediator of Brk in breast cancer (1), was dramatically increased during the involution timecourse in Brk transgenic mice. *In vitro* expression of Brk in HC11 cells promoted STAT5 and p38 MAPK activation, as well as anchorage independent survival in HC11 and HMEC cells. Remarkably, WAP-Brk mice develop tumors at a rate half that of wild-type mice, and they displayed the same pattern of STAT5 and p38 MAPK activation. Using breast tumor biopsies, we also identified the presence of STAT5 and p38 MAPK activation in Brk positive human tumors.

These results strongly suggest that Brk expression in non-transformed mammary epithelial cells promotes tumorigenesis, as opposed to differentiation, as it does in tissues that endogenously express Brk (38, 41). The $Ptk6^{-/-}$ mouse created by Haegebarth, et al.

(41) displayed no mammary phenotype at any developmental stage, indicating that Brk has no role in normal mammary gland biology. However, as Brk is expressed in most mammary cancers, there is a strong implication that Brk contributes to initiation or maintenance of malignancy in the breast. As ours is the first *in vivo* model to force Brk expression in the normally Brk-null mammary gland, it is promising that our results identified Brk mediated signaling events (STAT5 and p38 MAPK phosphorylation) that were conserved in non-transformed cell lines, mouse mammary glands, and human tumor biopsies.

As a complement to mouse modeling of breast cancer, *in vitro* models remain valuable tools for investigating mechanistic experiments. As such, we made an effort to recapitulate Brk-mediated biology in various *in vitro* assays. Culturing HMEC-Brk cells in Matrigel resulted in the formation hollow mammary organoids, similar to HMEC control cells (and normal mammary development). Interestingly, Brk expression in HMEC cells conferred partial resistance to the cytotoxic drug doxorubicin. As Brk is not expressed in normal mammary epithelial cells, we looked to cell models that endogenously express Brk, increasing the potential that "context appropriate" signaling modules are present. Intracellular Brk localization was differentially regulated in response to growth factor treatment of HaCaT keratinocytes and MDA-MB-231 breast cancer cells, suggesting that Brk has different signaling mechanisms in normal cells versus malignant cells. Brk mediated Erk5 and p38 MAPK phosphorylation occurs in response to HRG and EGF treatment in T47D and SKBR3 breast cancer cells. IL-1β treatment (an activator of p38 MAPK independent of GFRs) activated p38 MAPK in both

Brk knockdown and control cells, indicating specificity in ligand induced signaling activation.

Taken together, these *in vitro* assays of Brk mediated biology suggest a divergence in Brk mediated signaling, serving a differentiative or inhibitory role in normal tissues/cells, and an oncogenic role in cancer cells. However, it is likely that the proto-oncogenic role of Brk in normal tissues can co-opt signaling molecules (STAT5, p38 MAPK, Erk5) in order to become oncogenic. *In vitro* models of Brk expression in normal mammary epithelium are useful to delineate signaling mechanisms, and will likely be key in defining the shift of Brk signaling from proto-oncogenic to primarily oncogenic.

Fig. 5.1: Brk Signaling Summary

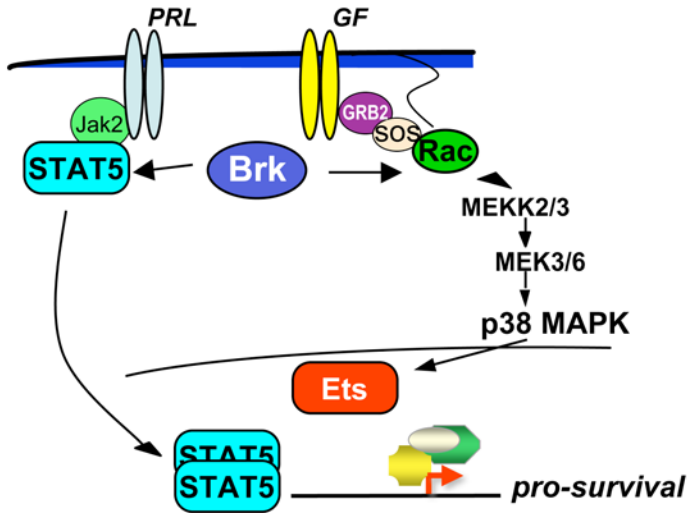

Figure 5.1. Brk mediates STAT5 and p38 MAPK signaling pathways to promote cellular survival. Prolactin and various growth factors activate STAT5 and p38 MAPK signaling pathways, likely upregulating transcription of pro-survival gene targets of STAT5 and the Ets family of transcription factors. In this thesis, Brk is implicated in promoting the phosphorylation and activation of these signaling pathways in normal mammary epithelium, delaying mammary involution and promoting tumorigenesis in a mouse model.

SIGNIFICANCE

PTKs are elevated in breast cancer, and as such, have become a focus for therapeutic development. In theory, Brk is a valuable target for breast cancer therapy, because it is expressed in up to 86% of breast cancers (1), but is not expressed in normal breast tissue. Brk expression in breast tumors is associated with the aggressive phenotype of high grade, invasive tumors (1, 21, 40) and confers resistance to the kinase inhibitor Lapatinib (37). However, understanding *how* Brk contributes to malignancy in breast cancer is still unclear. Delineating mechanisms by which Brk induces or supports oncogenic transformation may provide insight into how to target Brk for therapeutic gains. This work contributes to the understanding of Brk-mediated biology in normal mammary epithelium by 1) establishing a mouse model of Brk-mediated tumorigenesis and 2) identifying candidate signaling molecules and pathways that are activated by Brk expression which promote cellular survival and tumorigenesis in multiple models, both *in vitro* and *in vivo*. Additionally, studies were done that highlight the importance of the context (normal vs. cancer, *in vitro* vs. *in vivo*) in which Brk is expressed. Thus, utilization of these models of Brk expression in the normal mammary epithelium will allow Brk mediated mechanisms of tumorigenesis to be defined, and potentially extrapolated to assigning a role(s) for Brk in breast cancer progression.

REFERENCES

1. Ostrander JH, Daniel AR, Lofgren K, Kleer CG, Lange CA. Breast tumor kinase (protein tyrosine kinase 6) regulates heregulin-induced activation of ERK5 and p38 MAP kinases in breast cancer cells. Cancer Res 2007; 67: 4199-209.

2. Hennipman A, van Oirschot BA, Smits J, Rijksen G, Staal GE. Tyrosine kinase activity in breast cancer, benign breast disease, and normal breast tissue. Cancer Res 1989; 49: 516-21.

3. Bolla M, Rostaing-Puissant BR, Chedin M, et al. Protein tyrosine kinase activity as a prognostic parameter in breast cancer, a pilot study. Breast Cancer Res Treat 1993; 26: 283-7.

4. Liu X, Pawson T. Biochemistry of the Src protein-tyrosine kinase: regulation by SH2 and SH3 domains. Recent Prog Horm Res 1994; 49: 149-60.

5. Marshall CJ. Specificity of receptor tyrosine kinase signaling: transient versus sustained extracellular signal-regulated kinase activation. Cell 1995; 80: 179-85.

6. Schlessinger J. Cell signaling by receptor tyrosine kinases. Cell 2000; 103: 211-25.

7. Schlessinger J. New roles for Src kinases in control of cell survival and angiogenesis. Cell 2000; 100: 293-6.

8. Mitchell PJ, Barker KT, Martindale JE, et al. Cloning and characterisation of cDNAs encoding a novel non-receptor tyrosine kinase, brk, expressed in human breast tumours. Oncogene 1994; 9: 2383-90.

9. Siyanova EY, Serfas MS, Mazo IA, Tyner AL. Tyrosine kinase gene expression in the mouse small intestine. Oncogene 1994; 9: 2053-7.

10. Vasioukhin V, Serfas MS, Siyanova EY, et al. A novel intracellular epithelial cell tyrosine kinase is expressed in the skin and gastrointestinal tract. Oncogene 1995; 10: 349-57.

11. Lee ST, Strunk KM, Spritz RA. A survey of protein tyrosine kinase mRNAs expressed in normal human melanocytes. Oncogene 1993; 8: 3403-10.

12. Qiu H, Miller WT. Regulation of the nonreceptor tyrosine kinase Brk by autophosphorylation and by autoinhibition. J Biol Chem 2002; 277: 34634-41.

13. Serfas MS, Tyner AL. Brk, Srm, Frk, and Src42A form a distinct family of intracellular Src-like tyrosine kinases. Oncol Res 2003; 13: 409-19.

14. Lee H, Kim M, Lee KH, Kang KN, Lee ST. Exon-intron structure of the human PTK6 gene demonstrates that PTK6 constitutes a distinct family of non-receptor tyrosine kinase. Mol Cells 1998; 8: 401-7.

15. Kasprzycka M, Majewski M, Wang ZJ, et al. Expression and oncogenic role of Brk (PTK6/Sik) protein tyrosine kinase in lymphocytes. Am J Pathol 2006; 168: 1631-41.

16. Llor X, Serfas MS, Bie W, et al. BRK/Sik expression in the gastrointestinal tract and in colon tumors. Clin Cancer Res 1999; 5: 1767-77.

17. Derry JJ, Prins GS, Ray V, Tyner AL. Altered localization and activity of the intracellular tyrosine kinase BRK/Sik in prostate tumor cells. Oncogene 2003; 22: 4212-20.

18. Schmandt RE, Bennett M, Clifford S, et al. The BRK tyrosine kinase is expressed in high-grade serous carcinoma of the ovary. Cancer Biol Ther 2006; 5: 1136-41.

19. Lin HS, Berry GJ, Fee WE, Jr., Terris DJ, Sun Z. Identification of tyrosine kinases overexpressed in head and neck cancer. Arch Otolaryngol Head Neck Surg 2004; 130: 311-6.

20. Easty DJ, Mitchell PJ, Patel K, Florenes VA, Spritz RA, Bennett DC. Loss of expression of receptor tyrosine kinase family genes PTK7 and SEK in metastatic melanoma. Int J Cancer 1997; 71: 1061-5.

21. Chen HY, Shen CH, Tsai YT, Lin FC, Huang YP, Chen RH. Brk activates rac1 and promotes cell migration and invasion by phosphorylating paxillin. Mol Cell Biol 2004; 24: 10558-72.

22. Liu L, Gao Y, Qiu H, Miller WT, Poli V, Reich NC. Identification of STAT3 as a specific substrate of breast tumor kinase. Oncogene 2006; 25: 4904-12.

23. Weaver AM, Silva CM. Signal transducer and activator of transcription 5b: a new target of breast tumor kinase/protein tyrosine kinase 6. Breast Cancer Res 2007; 9: R79.

24. Liu X, Robinson GW, Hennighausen L. Activation of Stat5a and Stat5b by tyrosine phosphorylation is tightly linked to mammary gland differentiation. Mol Endocrinol 1996; 10: 1496-506.

25. Philp JA, Burdon TG, Watson CJ. Differential activation of STATs 3 and 5 during mammary gland development. FEBS Lett 1996; 396: 77-80.

26. Derry JJ, Richard S, Valderrama Carvajal H, et al. Sik (BRK) phosphorylates Sam68 in the nucleus and negatively regulates its RNA binding ability. Mol Cell Biol 2000; 20: 6114-26.

27. Mitchell PJ, Sara EA, Crompton MR. A novel adaptor-like protein which is a substrate for the non-receptor tyrosine kinase, BRK. Oncogene 2000; 19: 4273-82.

28. Ikeda O, Miyasaka Y, Sekine Y, et al. STAP-2 is phosphorylated at tyrosine-250 by Brk and modulates Brk-mediated STAT3 activation. Biochem Biophys Res Commun 2009; 384: 71-5.

29. Haegebarth A, Heap D, Bie W, Derry JJ, Richard S, Tyner AL. The nuclear tyrosine kinase BRK/Sik phosphorylates and inhibits the RNA-binding activities of the Sam68-like mammalian proteins SLM-1 and SLM-2. J Biol Chem 2004; 279: 54398-404.

30. Lukong KE, Richard S. Breast tumor kinase BRK requires kinesin-2 subunit KAP3A in modulation of cell migration. Cell Signal 2008; 20: 432-42.

31. Shen CH, Chen HY, Lin MS, et al. Breast tumor kinase phosphorylates p190RhoGAP to regulate rho and ras and promote breast carcinoma growth, migration, and invasion. Cancer Res 2008; 68: 7779-87.

32. Lukong KE, Huot ME, Richard S. BRK phosphorylates PSF promoting its cytoplasmic localization and cell cycle arrest. Cell Signal 2009; 21: 1415-22.

33. Palka-Hamblin HL, Gierut JJ, Bie W, et al. Identification of beta-catenin as a target of the intracellular tyrosine kinase PTK6. J Cell Sci; 123: 236-45.

34. Zheng Y, Peng M, Wang Z, Asara JM, Tyner AL. Protein tyrosine kinase 6 directly phosphorylates AKT and promotes AKT activation in response to epidermal growth factor. Mol Cell Biol; 30: 4280-92.

35. Kamalati T, Jolin HE, Mitchell PJ, et al. Brk, a breast tumor-derived non-receptor protein-tyrosine kinase, sensitizes mammary epithelial cells to epidermal growth factor. J Biol Chem 1996; 271: 30956-63.

36. Kamalati T, Jolin HE, Fry MJ, Crompton MR. Expression of the BRK tyrosine kinase in mammary epithelial cells enhances the coupling of EGF signalling to PI 3-kinase and Akt, via erbB3 phosphorylation. Oncogene 2000; 19: 5471-6.

37. Xiang B, Chatti K, Qiu H, et al. Brk is coamplified with ErbB2 to promote proliferation in breast cancer. Proc Natl Acad Sci U S A 2008; 105: 12463-8.

38. Vasioukhin V, Tyner AL. A role for the epithelial-cell-specific tyrosine kinase Sik during keratinocyte differentiation. Proc Natl Acad Sci U S A 1997; 94: 14477-82.

39. Castro NE, Lange CA. Breast tumor kinase and extracellular signal-regulated kinase 5 mediate Met receptor signaling to cell migration in breast cancer cells. Breast Cancer Res 2010; 12: R60.

40. Harvey AJ, Pennington CJ, Porter S, et al. Brk protects breast cancer cells from autophagic cell death induced by loss of anchorage. Am J Pathol 2009; 175: 1226-34.

41. Haegebarth A, Bie W, Yang R, et al. Protein tyrosine kinase 6 negatively regulates growth and promotes enterocyte differentiation in the small intestine. Mol Cell Biol 2006; 26: 4949-57.

42. Haegebarth A, Perekatt AO, Bie W, Gierut JJ, Tyner AL. Induction of protein tyrosine kinase 6 in mouse intestinal crypt epithelial cells promotes DNA damage-induced apoptosis. Gastroenterology 2009; 137: 945-54.

43. Sakakura T, Kusano I, Kusakabe M, Inaguma Y, Nishizuka Y. Biology of mammary fat pad in fetal mouse: capacity to support development of various fetal epithelia in vivo. Development 1987; 100: 421-30.

44. Robinson GW. Cooperation of signalling pathways in embryonic mammary gland development. Nat Rev Genet 2007; 8: 963-72.

45. Hennighausen L, Robinson GW. Information networks in the mammary gland. Nat Rev Mol Cell Biol 2005; 6: 715-25.

46. Robinson GW, McKnight RA, Smith GH, Hennighausen L. Mammary epithelial cells undergo secretory differentiation in cycling virgins but require pregnancy for the establishment of terminal differentiation. Development 1995; 121: 2079-90.

47. Ailhaud G, Grimaldi P, Negrel R. Cellular and molecular aspects of adipose tissue development. Annu Rev Nutr 1992; 12: 207-33.

48. Neville MC, Medina D, Monks J, Hovey RC. The mammary fat pad. J Mammary Gland Biol Neoplasia 1998; 3: 109-16.

49. Walker NI, Bennett RE, Kerr JF. Cell death by apoptosis during involution of the lactating breast in mice and rats. Am J Anat 1989; 185: 19-32.

50. Li M, Liu X, Robinson G, et al. Mammary-derived signals activate programmed cell death during the first stage of mammary gland involution. Proc Natl Acad Sci U S A 1997; 94: 3425-30.

51. Quaglino A, Salierno M, Pellegrotti J, Rubinstein N, Kordon EC. Mechanical strain induces involution-associated events in mammary epithelial cells. BMC Cell Biol 2009; 10: 55.

52. Heermeier K, Benedict M, Li M, Furth P, Nunez G, Hennighausen L. Bax and Bcl-xs are induced at the onset of apoptosis in involuting mammary epithelial cells. Mech Dev 1996; 56: 197-207.

53. Feng Z, Marti A, Jehn B, Altermatt HJ, Chicaiza G, Jaggi R. Glucocorticoid and progesterone inhibit involution and programmed cell death in the mouse mammary gland. J Cell Biol 1995; 131: 1095-103.

54. Wiens DJ, Brooks CL, Hodgson CP. Casein, actin, and tubulin expression during early involution in bovine and murine mammary tissue. J Dairy Sci 1992; 75: 1857-69.

55. Lund LR, Romer J, Thomasset N, et al. Two distinct phases of apoptosis in mammary gland involution: proteinase-independent and -dependent pathways. Development 1996; 122: 181-93.

56. Pullan S, Wilson J, Metcalfe A, et al. Requirement of basement membrane for the suppression of programmed cell death in mammary epithelium. J Cell Sci 1996; 109 (Pt 3): 631-42.

57. Talhouk RS, Bissell MJ, Werb Z. Coordinated expression of extracellular matrix-degrading proteinases and their inhibitors regulates mammary epithelial function during involution. J Cell Biol 1992; 118: 1271-82.

58. Strange R, Li F, Saurer S, Burkhardt A, Friis RR. Apoptotic cell death and tissue remodelling during mouse mammary gland involution. Development 1992; 115: 49-58.

59. Stein T, Morris JS, Davies CR, et al. Involution of the mouse mammary gland is associated with an immune cascade and an acute-phase response, involving LBP, CD14 and STAT3. Breast Cancer Res 2004; 6: R75-91.

60. O'Brien J, Lyons T, Monks J, et al. Alternatively activated macrophages and collagen remodeling characterize the postpartum involuting mammary gland across species. Am J Pathol; 176: 1241-55.

61. Monks J, Rosner D, Geske FJ, et al. Epithelial cells as phagocytes: apoptotic epithelial cells are engulfed by mammary alveolar epithelial cells and repress inflammatory mediator release. Cell Death Differ 2005; 12: 107-14.

62. Monks J, Smith-Steinhart C, Kruk ER, Fadok VA, Henson PM. Epithelial cells remove apoptotic epithelial cells during post-lactation involution of the mouse mammary gland. Biol Reprod 2008; 78: 586-94.

63. Atabai K, Fernandez R, Huang X, et al. Mfge8 is critical for mammary gland remodeling during involution. Mol Biol Cell 2005; 16: 5528-37.

64. Hanayama R, Nagata S. Impaired involution of mammary glands in the absence of milk fat globule EGF factor 8. Proc Natl Acad Sci U S A 2005; 102: 16886-91.

65. Bingle L, Brown NJ, Lewis CE. The role of tumour-associated macrophages in tumour progression: implications for new anticancer therapies. J Pathol 2002; 196: 254-65.

66. Clarkson RW, Wayland MT, Lee J, Freeman T, Watson CJ. Gene expression profiling of mammary gland development reveals putative roles for death receptors and immune mediators in post-lactational regression. Breast Cancer Res 2004; 6: R92-109.

67. Mantovani A, Sozzani S, Locati M, et al. Infiltration of tumours by macrophages and dendritic cells: tumour-associated macrophages as a paradigm for polarized M2 mononuclear phagocytes. Novartis Found Symp 2004; 256: 137-45; discussion 46-8, 259-69.

68. Van Ginderachter JA, Movahedi K, Hassanzadeh Ghassabeh G, et al. Classical and alternative activation of mononuclear phagocytes: picking the best of both worlds for tumor promotion. Immunobiology 2006; 211: 487-501.

69. Nusse R, van Ooyen A, Cox D, Fung YK, Varmus H. Mode of proviral activation of a putative mammary oncogene (int-1) on mouse chromosome 15. Nature 1984; 307: 131-6.

70. Nusse R, Varmus HE. Many tumors induced by the mouse mammary tumor virus contain a provirus integrated in the same region of the host genome. Cell 1982; 31: 99-109.

71. Dickson C, Smith R, Brookes S, Peters G. Tumorigenesis by mouse mammary tumor virus: proviral activation of a cellular gene in the common integration region int-2. Cell 1984; 37: 529-36.

72. Dickson C, Acland P, Smith R, et al. Characterization of int-2: a member of the fibroblast growth factor family. J Cell Sci Suppl 1990; 13: 87-96.

73. Stewart TA, Pattengale PK, Leder P. Spontaneous mammary adenocarcinomas in transgenic mice that carry and express MTV/myc fusion genes. Cell 1984; 38: 627-37.

74. Hennighausen L. Mouse models for breast cancer. Breast Cancer Res 2000; 2: 2-7.

75. Simons JP, McClenaghan M, Clark AJ. Alteration of the quality of milk by expression of sheep beta-lactoglobulin in transgenic mice. Nature 1987; 328: 530-2.

76. Harris S, McClenaghan M, Simons JP, Ali S, Clark AJ. Developmental regulation of the sheep beta-lactoglobulin gene in the mammary gland of transgenic mice. Dev Genet 1991; 12: 299-307.

77. Hennighausen LG, Sippel AE. Mouse whey acidic protein is a novel member of the family of 'four-disulfide core' proteins. Nucleic Acids Res 1982; 10: 2677-84.

78. Burdon T, Sankaran L, Wall RJ, Spencer M, Hennighausen L. Expression of a whey acidic protein transgene during mammary development. Evidence for different mechanisms of regulation during pregnancy and lactation. J Biol Chem 1991; 266: 6909-14.

79. Pittius CW, Sankaran L, Topper YJ, Hennighausen L. Comparison of the regulation of the whey acidic protein gene with that of a hybrid gene containing the whey acidic protein gene promoter in transgenic mice. Mol Endocrinol 1988; 2: 1027-32.

80. Pittius CW, Hennighausen L, Lee E, et al. A milk protein gene promoter directs the expression of human tissue plasminogen activator cDNA to the mammary gland in transgenic mice. Proc Natl Acad Sci U S A 1988; 85: 5874-8.

81. Pierce DF, Jr., Johnson MD, Matsui Y, et al. Inhibition of mammary duct development but not alveolar outgrowth during pregnancy in transgenic mice expressing active TGF-beta 1. Genes Dev 1993; 7: 2308-17.

82. Jhappan C, Geiser AG, Kordon EC, et al. Targeting expression of a transforming growth factor beta 1 transgene to the pregnant mammary gland inhibits alveolar development and lactation. EMBO J 1993; 12: 1835-45.

83. Ostrander JH, Daniel AR, Lange CA. Brk/PTK6 signaling in normal and cancer cell models. Curr Opin Pharmacol 2010.

84. Faivre EJ, Daniel AR, Hillard CJ, Lange CA. Progesterone receptor rapid signaling mediates serine 345 phosphorylation and tethering to specificity protein 1 transcription factors. Mol Endocrinol 2008; 22: 823-37.

85. Debnath J, Muthuswamy SK, Brugge JS. Morphogenesis and oncogenesis of MCF-10A mammary epithelial acini grown in three-dimensional basement membrane cultures. Methods 2003; 30: 256-68.

86. Tepera SB, McCrea PD, Rosen JM. A beta-catenin survival signal is required for normal lobular development in the mammary gland. J Cell Sci 2003; 116: 1137-49.

87. Budwit-Novotny DA, McCarty KS, Cox EB, et al. Immunohistochemical analyses of estrogen receptor in endometrial adenocarcinoma using a monoclonal antibody. Cancer Res 1986; 46: 5419-25.

88. Barker KT, Jackson LE, Crompton MR. BRK tyrosine kinase expression in a high proportion of human breast carcinomas. Oncogene 1997; 15: 799-805.

89. Chapman RS, Lourenco PC, Tonner E, et al. Suppression of epithelial apoptosis and delayed mammary gland involution in mice with a conditional knockout of Stat3. Genes Dev 1999; 13: 2604-16.

90. Radany EH, Hong K, Kesharvarzi S, Lander ES, Bishop JM. Mouse mammary tumor virus/v-Ha-ras transgene-induced mammary tumors exhibit strain-specific allelic loss on mouse chromosome 4. Proc Natl Acad Sci U S A 1997; 94: 8664-9.

91. Evers B, Jonkers J. Mouse models of BRCA1 and BRCA2 deficiency: past lessons, current understanding and future prospects. Oncogene 2006; 25: 5885-97.

92. Muller WJ, Sinn E, Pattengale PK, Wallace R, Leder P. Single-step induction of mammary adenocarcinoma in transgenic mice bearing the activated c-neu oncogene. Cell 1988; 54: 105-15.

93. Schwertfeger KL, Richert MM, Anderson SM. Mammary gland involution is delayed by activated Akt in transgenic mice. Mol Endocrinol 2001; 15: 867-81.

94. Jager R, Herzer U, Schenkel J, Weiher H. Overexpression of Bcl-2 inhibits alveolar cell apoptosis during involution and accelerates c-myc-induced tumorigenesis of the mammary gland in transgenic mice. Oncogene 1997; 15: 1787-95.

95. Brandt R, Eisenbrandt R, Leenders F, et al. Mammary gland specific hEGF receptor transgene expression induces neoplasia and inhibits differentiation. Oncogene 2000; 19: 2129-37.

96. Lazar H, Baltzer A, Gimmi C, Marti A, Jaggi R. Over-expression of erbB-2/neu is paralleled by inhibition of mouse-mammary-epithelial-cell differentiation and developmental apoptosis. Int J Cancer 2000; 85: 578-83.

97. Leung K, Nagy A, Gonzalez-Gomez I, Groffen J, Heisterkamp N, Kaartinen V. Targeted expression of activated Rac3 in mammary epithelium leads to defective

postlactational involution and benign mammary gland lesions. Cells Tissues Organs 2003; 175: 72-83.

98. Baxter FO, Neoh K, Tevendale MC. The beginning of the end: death signaling in early involution. J Mammary Gland Biol Neoplasia 2007; 12: 3-13.

99. Marti A, Graber H, Lazar H, et al. Caspases: decoders of apoptotic signals during mammary involution. Caspase activation during involution. Adv Exp Med Biol 2000; 480: 195-201.

100. Liu X, Robinson GW, Wagner KU, Garrett L, Wynshaw-Boris A, Hennighausen L. Stat5a is mandatory for adult mammary gland development and lactogenesis. Genes Dev 1997; 11: 179-86.

101. Schmitt-Ney M, Happ B, Ball RK, Groner B. Developmental and environmental regulation of a mammary gland-specific nuclear factor essential for transcription of the gene encoding beta-casein. Proc Natl Acad Sci U S A 1992; 89: 3130-4.

102. Gouilleux F, Wakao H, Mundt M, Groner B. Prolactin induces phosphorylation of Tyr694 of Stat5 (MGF), a prerequisite for DNA binding and induction of transcription. EMBO J 1994; 13: 4361-9.

103. Esteva FJ, Sahin AA, Smith TL, et al. Prognostic significance of phosphorylated P38 mitogen-activated protein kinase and HER-2 expression in lymph node-positive breast carcinoma. Cancer 2004; 100: 499-506.

104. Ball RK, Friis RR, Schoenenberger CA, Doppler W, Groner B. Prolactin regulation of beta-casein gene expression and of a cytosolic 120-kd protein in a cloned mouse mammary epithelial cell line. EMBO J 1988; 7: 2089-95.

105. Danielson KG, Oborn CJ, Durban EM, Butel JS, Medina D. Epithelial mouse mammary cell line exhibiting normal morphogenesis in vivo and functional differentiation in vitro. Proc Natl Acad Sci U S A 1984; 81: 3756-60.

106. Merlo GR, Graus-Porta D, Cella N, Marte BM, Taverna D, Hynes NE. Growth, differentiation and survival of HC11 mammary epithelial cells: diverse effects of receptor tyrosine kinase-activating peptide growth factors. Eur J Cell Biol 1996; 70: 97-105.

107. Irie HY, Shrestha Y, Selfors LM, et al. PTK6 regulates IGF-1-induced anchorage-independent survival. PLoS One 2010; 5: e11729.

108. Born M, Quintanilla-Fend L, Braselmann H, et al. Simultaneous over-expression of the Her2/neu and PTK6 tyrosine kinases in archival invasive ductal breast carcinomas. J Pathol 2005; 205: 592-6.

109. Radisky DC, Hartmann LC. Mammary involution and breast cancer risk: transgenic models and clinical studies. J Mammary Gland Biol Neoplasia 2009; 14: 181-91.

110. Walker SR, Nelson EA, Zou L, et al. Reciprocal effects of STAT5 and STAT3 in breast cancer. Mol Cancer Res 2009; 7: 966-76.

111. Clarkson RW, Boland MP, Kritikou EA, et al. The genes induced by signal transducer and activators of transcription (STAT)3 and STAT5 in mammary epithelial cells define the roles of these STATs in mammary development. Mol Endocrinol 2006; 20: 675-85.

112. Demidov ON, Kek C, Shreeram S, et al. The role of the MKK6/p38 MAPK pathway in Wip1-dependent regulation of ErbB2-driven mammary gland tumorigenesis. Oncogene 2007; 26: 2502-6.

113. Cuevas BD, Abell AN, Johnson GL. Role of mitogen-activated protein kinase kinase kinases in signal integration. Oncogene 2007; 26: 3159-71.

114. Wang RA, Zhang H, Balasenthil S, Medina D, Kumar R. PAK1 hyperactivation is sufficient for mammary gland tumor formation. Oncogene 2006; 25: 2931-6.

115. Chen L, Mayer JA, Krisko TI, et al. Inhibition of the p38 kinase suppresses the proliferation of human ER-negative breast cancer cells. Cancer Res 2009; 69: 8853-61.

116. Huang P, Duda DG, Jain RK, Fukumura D. Histopathologic findings and establishment of novel tumor lines from spontaneous tumors in FVB/N mice. Comp Med 2008; 58: 253-63.

117. Wang TC, Jee SH, Tsai TF, Huang YL, Tsai WL, Chen RH. Role of breast tumour kinase in the in vitro differentiation of HaCaT cells. Br J Dermatol 2005; 153: 282-9.

118. Vekemans M, Delvoye P, L'Hermite M, Robyn C. Serum prolactin levels during the menstrual cycle. J Clin Endocrinol Metab 1977; 44: 989-93.

119. Kleinman HK, McGarvey ML, Liotta LA, Robey PG, Tryggvason K, Martin GR. Isolation and characterization of type IV procollagen, laminin, and heparan sulfate proteoglycan from the EHS sarcoma. Biochemistry 1982; 21: 6188-93.

120. Haegebarth A, Clevers H. Wnt signaling, lgr5, and stem cells in the intestine and skin. Am J Pathol 2009; 174: 715-21.

121. Ie Kim H, Lee ST. Oncogenic functions of PTK6 are enhanced by its targeting to plasma membrane but abolished by its targeting to nucleus. J Biochem 2009; 146: 133-9.

122. Faivre EJ, Lange CA. Progesterone receptors upregulate Wnt-1 to induce epidermal growth factor receptor transactivation and c-Src-dependent sustained activation of Erk1/2 mitogen-activated protein kinase in breast cancer cells. Mol Cell Biol 2007; 27: 466-80.

123. Nelson CM, Bissell MJ. Of extracellular matrix, scaffolds, and signaling: tissue architecture regulates development, homeostasis, and cancer. Annu Rev Cell Dev Biol 2006; 22: 287-309.

124. Gallego MI, Bierie B, Hennighausen L. Targeted expression of HGF/SF in mouse mammary epithelium leads to metastatic adenosquamous carcinomas through the activation of multiple signal transduction pathways. Oncogene 2003; 22: 8498-508.

125. Parmar H, Cunha GR. Epithelial-stromal interactions in the mouse and human mammary gland in vivo. Endocr Relat Cancer 2004; 11: 437-58.

126. Ferrell JE, Jr. How regulated protein translocation can produce switch-like responses. Trends Biochem Sci 1998; 23: 461-5.

127. Mitchell PJ, Barker KT, Shipley J, Crompton MR. Characterisation and chromosome mapping of the human non receptor tyrosine kinase gene, brk. Oncogene 1997; 15: 1497-502.

128. Brauer PM, Zheng Y, Wang L, Tyner AL. Cytoplasmic retention of protein tyrosine kinase 6 promotes growth of prostate tumor cells. Cell Cycle; 9: 4190-9.

129. Haegebarth A, Nunez R, Tyner AL. The intracellular tyrosine kinase Brk sensitizes non-transformed cells to inducers of apoptosis. Cell Cycle 2005; 4: 1239-46.

130. Kuperwasser C, Chavarria T, Wu M, et al. Reconstruction of functionally normal and malignant human breast tissues in mice. Proc Natl Acad Sci U S A 2004; 101: 4966-71.

131. Miyamoto S, Teramoto H, Gutkind JS, Yamada KM. Integrins can collaborate with growth factors for phosphorylation of receptor tyrosine kinases and MAP kinase activation: roles of integrin aggregation and occupancy of receptors. J Cell Biol 1996; 135: 1633-42.